polyclonal anti-ERK-1/2 antibody (Ab) was from Cell Signaling Technology (Beverly, MA, USA). Rabbit polyclonal anti-Flt3 Ab was from Santa Cruz Biotechnology (Santa Cruz, CA, USA). PKC412 was obtained from Novartis Pharmaceuticals (Basel, Switzerland). 12-*O*-tetradecyanoylphorbol 13-acetate (PMA) and 1,25-dihydroxy vitamin D3 (Vit.D3) were from Sigma (St Louis, MO, USA). Fibrinogen (FB) was from Calbiochem (San Diego, CA, USA).

Cell lines and cell culture

The murine pro-B cell line, Ba/F3 cells and the murine myeloid progenitor cell line, 32Dcl.3 (32D) cells were maintained in RPMI 1640 containing 10% fetal calf serum (FCS), penicillin/streptomycin and 1 ng/ml rmIL-3. The murine B-cell lymphoma line, WEHI-231 (WEHI) cells were cultured in RPMI 1640 containing 10% FCS, 50 mM 2-mercaptoethanol and penicillin/streptomycin. The human leukemia cell lines, U937 and HL-60 cells, were maintained in RPMI 1640 containing 10% FCS, penicillin/streptomycin. An ecotropic retrovirus packaging cell line, Plat-E cells, was maintained in Dulbecco's modified Eagle's medium containing 10% FCS, 1 μg/ml puromycin (Sigma) and 10 μg/ml blasticidin S (Funakoshi Co., Tokyo, Japan).

DNA constructs and retroviral transfection

The construction of pMKIT-Neo vectors containing Flt3-wild type (WT) or Flt3-ITD and the transfection of Ba/F3 cells with these vectors were described previously.[39] The Flt3-D835V and Flt3-D835Y constructs were amplified by two-step polymerase chain reaction (PCR) from Flt3-WT in pMKIT-Neo vector using PFU DNA polymerase (Stratagene, La Jolla, CA, USA). Primers used in step 1 were: forward Flt3-*Bam*HI: 5′-CGCGGATCCATG GGCCCAGGAGTTCTG-3′, reverse Flt3-D835V: 5′-CATGATAA CGCGTGCCAATTCAAA-3′ or reverse Flt3-D835Y: 5′-GAATCA CTCATGATATATCGAGC-3′. Primers used in step 2 were: forward Flt3-D835V: 5′-TTTGGATTGGCACGCGTTATCATG-3′ or forward Flt3-D835Y: 5′-GCTCGATATATCATGAGTGATTC-3′, reverse Flt3-*Xba*I: 5′-GCTCTAGACTACGAATCTTCGACC TG-3′. PCR products from step 1 and step 2 were diluted and combined as templates using Flt3-*Bam*HI and Flt3-*Xba*I as the forward or reverse primers, respectively, to create mutant fragments, which were then subcloned into the pMKIT-Neo expression vector. For generation of stably transfected 32D cells, the sequence of Flt3-WT, Flt3-ITD, Flt3-D835V or Flt3-D835Y excised from pMKIT-Neo was subcloned into pMXs-IERS-Neomycin (pMXs-IN) retroviral vector.[40] The Plat-E packaging cells were transfected with these vectors by FuGENE 6 transfection reagent (Roche Diagnostics, Indianapolis, IN, USA) as described previously.[40] The retroviruses were used to infect 32D cells in the presence of rmIL-3. Stable transfectants were then selected with 1 mg/ml G418 (Nacalai Tesque Inc., Kyoto, Japan) for 2 weeks. Ba/F3 and 32D transfectants expressing Flt3-ITD, Flt3-D835V or Flt3-D835Y were maintained in RPMI 1640 containing 10% FCS in the absence of rmIL-3, while Flt3-WT-expressing cells were maintained in the presence of 10 ng/ml rhFL. The coding sequence of mouse TSC-22 was amplified by PCR from complementary DNA (cDNA) of Ba/F3 cells using AmpliTaq Gold (Roche Molecular Systems Inc., Branchburg, NJ, USA) and subcloned into pMXs-IERS-Puromycin (pMXs-IP) retroviral vectors.[40] A truncated TSC-22-LZ was amplified by PCR from plasmid, pEGFP-TSC-22-LZ (kindly provided by Hitoshi Kawamata, School of Medicine, Dokkyo University, Japan) and subcloned into pMXs-IP retroviral vectors. TSC-22-LZ contains TSC-box and leucine zipper, but not both repressor domains (RD). For retroviral transduction of TSC-22 into Ba/F3, 32D, WEHI, U937, HL-60 cells or Flt3-ITD-expressing cells, Plat-E packaging cells were transfected with pMXs-IP, pMXs-TSC-22-IP or pMXs-TSC-22-LZ-IP construct before infection with retroviruses. To avoid clonal differences as well as a bias by the selection in the absence of IL-3, pooled transfectants were selected with 2 μg/ml puromycin for 2 weeks and were subjected to experiments. These procedures were performed multiple times with the similar results.

Microarray analysis

Ba/F3 transfectants expressing Flt3-ITD or Flt3-D835V were maintained in the absence of rmIL-3. Total RNA was extracted by Trizol reagent (Invitrogen, Carlsbad, CA, USA) according to the manufacturer's protocol. Double-stranded cDNA was synthesized from 5 μg of total RNA with oligo $(dT)_{24}$ T7 primer, amplified with T7 RNA polymerase up to approximately 50 μg of cRNA, and hybridized to Affymetrix Mouse Expression array 430A, which contains 45 000 probe sets for 39 000 transcripts and variants from over 34 000 well-characterized mouse genes (Affymetrix, Santa Clara, CA, USA). After washing and staining, the arrays were scanned on the GeneChip system confocal scanner (Affymetrix, Hewlett-Packard, Santa Clara, CA, USA). The intensity for each feature of the array was captured with Affymetrix Microarray Suite (MAS) Version 5.0 software.

Real-time reverse transcription-PCR

Real-time reverse transcription-PCR was performed using a LightCycler Workflow System (Roche Diagnostics, Mannheim, Germany). cDNA was synthesized and amplified from 200 ng of RNA using a LightCycler FastStart DNA Master SYBR Green I kit (Roche Diagnostics). Reaction was subject to 45 cycles of PCR at 95°C for 10 s, 55°C for 10 s and 72°C for 20 s. All samples were independently analyzed at least three times. The following primer pairs were used: 5′-ATGAAATCCCAATGGTGTAGA-3′ (TSC-22 forward), 5′-CTATGCGGTTGATCCTGAGCC-3′ (TSC-22 reverse). The housekeeping gene, glyceraldehyde-3-phosphate dehydrogenase (GAPDH), served as an additional control for cDNA quality. Relative gene expression levels were calculated using standard curves generated by serial dilutions of cDNA of Ba/F3 cells or 32D cells. Product quality was checked by melting curve analysis via LightCycler software (Roche Diagnostics). Expression levels for each gene were divided by the GAPDH RNA expression level.

siRNA transfection

An Flt3-specific SMARTPool and Nonspecific control small interfering RNA (siRNA) were purchased from Dharmacon (Lafayette, CO, USA). For transfection, 5×10^6 cells were resuspended in the specific Nucleofector Solution V, mixed with 2.5 μg double-stranded siRNA targeting Flt3 mRNA or control siRNA, and nucleofected with the cell-specific program X-001 using the Amaxa Nucleofector Device (Amaxa, Gaithersburg, MD, USA), according to the manufacturer's protocols. Cells were analyzed 24 h after transfection by western blot and flow cytometry analysis.

Generation of anti-TSC-22 antibody

Purification of recombinant TSC-22 protein and generation of anti-TSC-22 polyclonal antibody was performed as described previously.[37] Briefly, a cDNA for the mouse TSC-22 was subcloned in the correct reading frame into pGEX4T-1

(Amersham Biosciences, Uppsala, Sweden) and verified by sequencing. glutathione *S*-transferase (GST)–TSC-22 was expressed in *Escherichia coli* strain BL21 (DE3) cultured with 100 mM lactose analog isopropylβ-D-thiogalactoside. GST-fusion proteins were purified by glutathione-sepharose 4B according to the standard protocols (Amersham Biosciences). Anti-TSC-22 polyclonal antibody was generated from the serum of immunized rabbit using purified GST–TSC-22 fusion protein (SCRUM Inc., Tokyo, Japan). In western blot analysis, this antibody detected two bands, the large of which corresponded to the full-length protein in size.

Immunoprecipitation and western blot analysis

Cells were lysed in lysis buffer (10% glycerol, 150 mM NaCl, 50 mM Tris-HCl at pH7.5, 1% NP-40) containing protease and phosphatase inhibitor cocktail tablets (Sigma), and then cell lysates were clarified by centrifugation. The protein concentration of the supernatants was determined with a Bio-Rad Protein Assay kit (Rio-Rad, Hercules, CA, USA). For immunoprecipitation, equivalent amounts of protein were incubated with anti-TSC-22 antibody and protein G Sepharose at 4°C for 2 h. The immunoprecipitates were washed four times with lysis buffer, then resuspended in sodium dodecyl sulfate (SDS) sample buffer and heated at 95°C for 5 min. Cell lysates or immunoprecipitates were separated by SDS-polyacrylamide gel electrophoresis gel (Wako, Osaka, Japan). Gels were transferred onto Immobilon membranes (Millpore, Bedford, MA, USA) and immunostained with an anti-TSC-22 Ab, anti-Flt3 Ab or anti-ERK Ab, followed by a horseradish peroxidase-labeled secondary Ab. Stained protein was visualized by chemiluminescence using ECL reagents (Amersham Biosciences).

Flow cytometry

Cells were washed with phosphate-buffered saline (PBS)/2% FCS, blocked with mouse FcBlock (BD Biosciences, Franklin Lakes, NJ, USA) for 15 min, and stained with the indicated antibodies for 20 min. After washing, cells were analyzed using a FACSCalibur flow cytometer with CellQuest software (BD Biosciences).

Analysis of cell growth

The cells were resuspended in RPMI 1640 including 10% FCS with or without indicated growth factors, and 1×10^3 cells were seeded into 96-well plates (Corning, NY, USA). After incubation for the indicated time at 37°C, cell growth was estimated by quantitating luminescence from the 96-well plates using CellTiter-Glo (Promega, Madison, WI, USA) and a Micro Lumat Plus luminometer (EG&G Berthold), according to the manufacturer's instructions. Briefly, the luminescence is recorded with a luminometer measuring the amount of ATP which is proportional to viable cell number.

Adhesion assay

Adhesion assay was performed as described previously.[41] In brief, the 96-well plates (Corning) were coated with 20 μg/ml FB in PBS for 1 h at 37°C, washed three times with PBS, blocked with 3% bovine serum albumin (BSA)/PBS for 1 h at 37°C, and washed three times with RPMI 1640. Cells were resuspended with the RPMI 1640 containing 10% FCS and transferred into coated wells with or without 1 ng/ml rmIL-3. The plates were incubated at 37°C for 2 h, and the unbound cells were washed away. Input and bound luminescence were directly quantitated from the 96-well plates using CellTiter-Glo and a Micro Lumat Plus luminometer. The percent of adhesion was calculated by dividing bound luminescence by input luminescence.

The evaluation of cell differentiation

U937 and HL-60 cells were seeded at 3×10^5 cells/ml and treated with 10 ng/ml PMA or 10 nM Vit.D3 for the indicated time. Surface expression level of CD11b, CD14, CD80 or HLA-DR was estimated by flow cytometry. Cells of cytocentrifuged by Shandon Cytopsin (Thermo Fisher SCIENTIFIC, Waltham, MA, USA) were stained with May-Grunwald-Giemsa and evaluated morphologically.

Mice

Eight-week-old male Balb/c mice or C3H/HeJ mice were purchased from Charles River Japan Inc. Mice were kept under standard laboratory conditions according to the guidelines of the Laboratory Animal Research Center, The Institute of Medical Science, The University of Tokyo. The transduced Ba/F3 cells (1×10^6 cells) or 32D cells (1×10^5 cells) were injected into the lateral tail vein of Balb/c or syngeneic C3H/HeJ mice, respectively. The injected mice (five mice in each group) were monitored daily. This study was approved by the Institutional Ethics Committee for Laboratory Animals Used in Experimental Research.

Statistical analysis

Statistical significance was calculated using the Student *t*-test for independent variables with Excel (Microsoft). *P*-values < 0.05 were considered statistically significant.

Results

Leukemia-like disease was rapidly induced by Flt3-ITD-transduced Ba/F3 cells but not by Flt3-D835V-transduced Ba/F3 cells

As reported, both Flt3-ITD and Flt3-TKD led to factor-independent growth of the transduced Ba/F3 cells.[9,14,15,17] We next investigated the leukemogenic potential of the transduced Ba/F3 cells by injecting them into syngeneic Balb/c mice. All the mice receiving the Flt3-ITD-transduced cells developed a lethal hematopoietic disease with a median latency period of approximately 8–9 weeks (Figure 1a). In contrast, only four of 10 mice receiving the Flt3-D835V-transduced cells developed a similar disease, with a longer latency period of 10–12 weeks. The remaining six mice were as healthy as the mice given an injection of the Flt3-WT-transduced cells during an extended observation time of 120 days. Histopathological analysis of the mice inoculated with Flt3-ITD-transduced cells revealed marked pathological findings. The expansion and infiltration of leukemia-like cells observed in liver and bone marrow confirmed the strong transforming ability of the Ba/F3 cells expressing Flt3-ITD (data not shown).

TSC-22 is highly expressed in Flt3-TKD-transduced cells but not in Flt3-ITD-transduced cells

The different phenotypes observed in transplantation experiments using the Flt3-ITD- or Flt3-D835V-transduced Ba/F3 cells prompted us to investigate the underlying molecular mechanisms. We hypothesized that the changes in gene expression patterns induced by Flt3-ITD or Flt3-D835V might reflect the

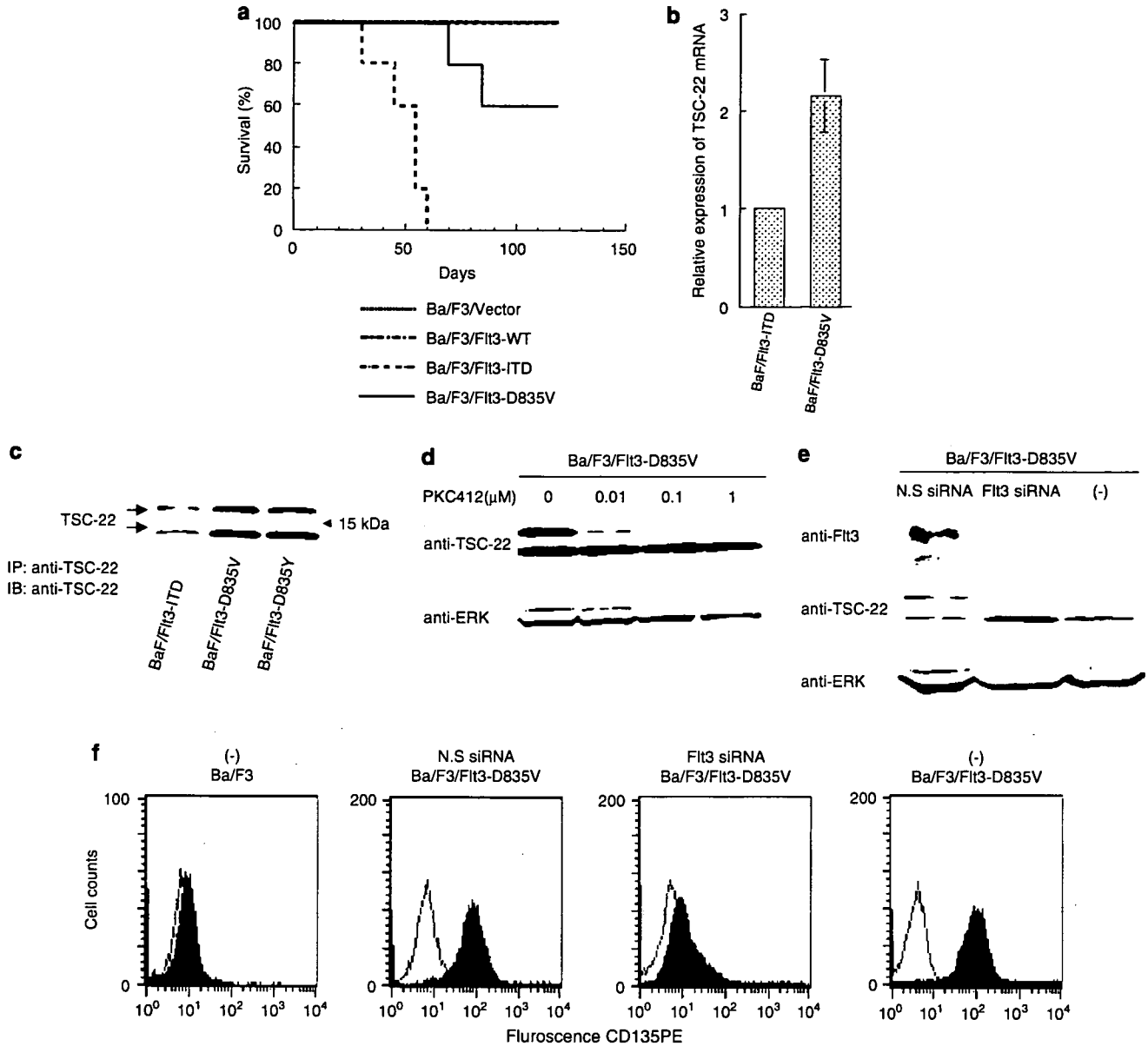

Figure 1 *In vivo* and *in vitro* effects of Flt3-ITD and Flt3-D835V. (**a**) Kaplan–Meier plot of survival. Balb/c mice ($n=5$ for each group) were injected via tail veins with 1×10^6 Ba/F3 cells expressing Flt3-WT, Flt3-ITD, Flt3-D835V and vector as control. Mouse survival was monitored daily for 120 days. The percentage of surviving mice (*y* axis) is plotted over the time after injection (*x* axis). This graph presents data from two independent experiments. (**b**) Quantification of TSC-22 mRNA levels in Ba/F3 cells by real-time RT-PCR. Total RNA was isolated from Ba/F3 transfectants under the same conditions as shown in Table 1. The bar represents the ratios of GAPDH-normalized expression values. Each bar represents the mean of three independent experiments. (**c**) Expression levels of TSC-22 protein in Ba/F3 transfectants. Equivalent amounts of cell extracts prepared from Ba/F3 transfectants were immunoprecipitated with anti-TSC-22 antibody, followed by immunoblotting with the same antibody. (**d**) Downregulation of TSC-22 by an Flt3 inhibitor PKC412. Flt3-D835V-expressing BaF3 cells were incubated with the indicated concentrations of PKC412 for 24 h in the absence of rmIL-3. Equivalent amounts of cell lysates were immunoblotted with anti-ERK Ab or immunoprecipitated with anti-TSC-22Ab, followed by immunoblotting with the same Ab. (**e–f**) Flt3 siRNA-induced downregulation of TSC-22. Flt3-D835V-expressing BaF3 cells were nucleofected with Flt3 or nonspecific control siRNA in the absence of rmIL-3. Expression of Flt3-D835V was determined (**e**) by immunoblotting of equivalent amounts of total cell lysates with anti-Flt3 Ab or (**f**) by flow cytometry analysis using isotype control mAb (blank areas) and PE-conjugated anti-CD135 mAb (filled areas) 24 h after siRNA transfection. Expression of TSC-22 or ERK was determined as described above. Ab, antibody; ERK, extracellular regulated kinase; GAPDH, glyceraldehyde-3-phosphate dehydrogenase; mAb, monoclonal antibody; PE, phycoerythrin; RT-PCR, reverse transcription-PCR; siRNA, small interfering RNA; TSC-22, TGF-β-stimulated clone-22.

different phenotypes during leukemogenesis. Therefore, we analyzed the gene expression profiles of Ba/F3 cells expressing Flt3-ITD or Flt3-D835V by microarray experiments. We chose the genes that were up- or downregulated at least twofold between the cells expressing Flt3-ITD versus Flt3-D835V (Table 1). Among them, we focused on one of the genes upregulated in Flt3-D835V-expressing cells, TSC-22, because it is known to be a tumor suppressor involved in the induction of apoptosis.

First, we quantified expression levels of TSC-22 mRNA by real-time PCR and confirmed that the Flt3-ITD-transduced Ba/F3 cells expressed a lower level of TSC-22 mRNA when compared with Flt3-D835V-transduced Ba/F3 cells (Figure 1b). Thus, the real-time PCR results were consistent with the microarray data

Table 1 Expression of genes regulated by Flt3-ITD and Flt3-D835V

Gene symbol	*Gene description*	*Average difference*	
		Flt3-ITD	*Flt3-D835V*
Increased by Flt3-ITD			
Ms4a3	Membrane-spanning 4-domains, subfamily A, member 3	204	100.4
Bnip3	BCL2/adenovirus E1B 19kDa-interacting protein 1, NIP3	226.5	80.6
Cd47	CD47 antigen (Rh-related antigen, integrin-associated signal transducer)	248.3	105
Enh-pending	Enigma homolog (R. norvegicus)	265.2	107.6
Podxl	podocalyxin-like	303.9	142.4
Csf2rb1	Colony stimulating factor 2 receptor, beta 1, low-affinity (granulocyte-macrophage)	355.3	162.8
Hba-a1	Hemoglobin alpha, adult chain 1	423.1	150.2
Serpina3g	Serine (or cysteine) proteinase inhibitor, clade A, member 3G	475.3	49.7
Tcrg-V4	T-cell receptor gamma, variable 4	501.1	182.6
Cd53	CD53 antigen	549.3	268.2
Csf2rb2	Colony stimulating factor 2 receptor, beta 2, low-affinity (granulocyte-macrophage)	861.1	349.6
Decreased by Flt3-D835V			
Tgfb1i4 (TSC-22)	Transforming growth factor beta 1 induced transcript 4	124.5	279.2
Hbb-b1	Hemoglobin, beta adult major chain	288.7	817.9

Changes in gene expression in Ba/F3 cells expressing Flt3-ITD and Flt3-D835V. RNAs harvested from Ba/F3 transfectants without cytokines were hybridized to mouse expression array. Only genes with fold differences of raw data >2 are listed.

described above. Next, we examined whether the change in mRNA levels correlated with that in protein levels. Since Flt3-D835Y is most frequently found among Flt3-TKD mutations, we examined the expression levels of TSC-22 in the cell lysates prepared from Flt3-D835Y-expressing Ba/F3 cells in addition to Flt3-ITD- and Flt3-D835V-expressing Ba/F3 cells. Immunoprecipitated lysate with anti-TSC-22 Ab was subject to immunoblotting for TSC-22. As shown in Figure 1c, western blot analysis revealed higher expression of TSC-22 in Flt3-D835V- and Flt3-D835Y-expressing cells compared to that in Flt3-ITD-expressing cells. To explore whether the kinase activity of Flt3-TKD is required for upregulation of TSC-22, we treated Flt3-D835V-expressing Ba/F3 cells with increasing concentrations of a known Flt3 inhibitor PKC412 for 24 h in the absence of rmIL-3.[42] As shown in Figure 1d, PKC412 dose-dependently decreased protein expression levels of a full length of TSC-22, while it did not affect expression level of ERK1/2 used as a control. Moreover, to determine whether sufficient expression levels of Flt3-TKD is indispensable for upregulation of TSC-22, we performed experiments to downregulate Flt3-D835V by transfecting Flt3 siRNA into Flt3-D835V-expressing Ba/F3 cells.[43] Flt3 siRNA, but not control siRNA, strongly inhibited the expression of Flt3-D835V at protein levels 24 h after transfection, although it did not affect that of ERK1/2 (Figure 1e). At the same time, flow cytometry analysis clearly demonstrated a drastic reduction of surface expression levels of Flt3-D835V by Flt3 siRNA, but no by control siRNA (Figure 1f). Importantly, a full length of TSC-22 was strongly inhibited in accordance with downregulation of Flt3-D835 by siRNA (Figure 1e). Collectively, sufficient expression and kinase activity of Flt3-TKD was indispensable for upregulation of TSC-22.

To further confirm if these data generally applied to hematopoietic cell lines, another murine myeloid cell line, 32D, was stably transfected with either Flt3-WT, Flt3-ITD, Flt3-D835V or Flt3-D835Y construct. Flow cytometry analysis revealed that the surface expression levels of Flt3-ITD, Flt3-D835V and Flt3-D835Y were comparable, but slightly lower than that of Flt3-WT and higher than that of endogenous Flt3 (Figure 2a). Then, we analyzed TSC-22 expression at both mRNA and protein levels. In accordance with the data using Ba/F3 cells, the expression level of TSC-22 in Flt3-ITD-ransduced 32D cells was significantly lower than those of Flt3-D835V- and Flt3-D835Y-transduced 32D cells in the presence of rmIL-3 (Figures 2b and c). Then, we compared the growth of 32D cells carrying either Flt3-ITD, Flt3-D835V or Flt3-D835Y. As reported, Flt3-ITD-, Flt3-D835V- and Flt3-D835Y-transduced 32D cells proliferated independently of an exogenous growth factor IL-3, although Flt3-D835V- and Flt3-D835Y-expressing cells showed a weaker proliferative response than Flt3-ITD-expressing cells (Figure 2d). Taken together, while both Flt3-ITD and Flt3-TKD induced factor-independent growth of 32D cells, upregulation of TSC-22 expression was observed only in the cells transduced with Flt3-D835V and Flt3-D835Y but not those transduced with Flt3-ITD. We postulated that the lower expression levels of TSC-22 might be associated with the higher rate of cell proliferation, resulting in the rapid induction of leukemia-like disease by Flt3-ITD-carrying cells.

Forced expression of TSC-22 inhibits cell growth in several leukemia-derived cell lines

To further evaluate the effects of TSC-22 on cell proliferation, we transduced TSC-22 or its dominant-negative form TSC-22-LZ into several leukemia-derived cell lines, including 32D, WEHI or U937 cells. TSC-22-LZ containing TSC-box and leucine zipper but not two RD has been reported to act as a dominant-negative inhibitor.[44] Flow cytometry analysis revealed that the surface expression levels of transduced-Flt3 isoforms were not altered with or without transduced-TSC-22 in 32D cells (Figure 3a). Enforced expression of TSC-22 or TSC-22LZ was confirmed by western blot using an anti-TSC-22 mAb (data not shown). As shown in Figure 3b (left panel), IL-3-dependent growth of 32D cells was significantly inhibited or accelerated by exogenous expression of TSC-22 or TSC-22-LZ, respectively. Interestingly, autonomous growth of Flt3-ITD-transduced 32D cells was significantly inhibited by exogenous expression of TSC-22 as shown in Figure 3b (right panel), while growth of Flt3-TKD-transduced 32D cells was accelerated by forced expression of TSC-22-LZ as shown in Figure 3d. Intriguingly, enforced expression of TSC-22 significantly inhibited the growth of Flt3-ITD-expressing cells down to the growth rate of Flt3-D835V-expressing cells (Figure 3e). We also demonstrated similar effects of TSC-22 on the growth of WEHI and U937 cells (Figure 3c). To next examine the *in vivo* effect of TSC-22 on the

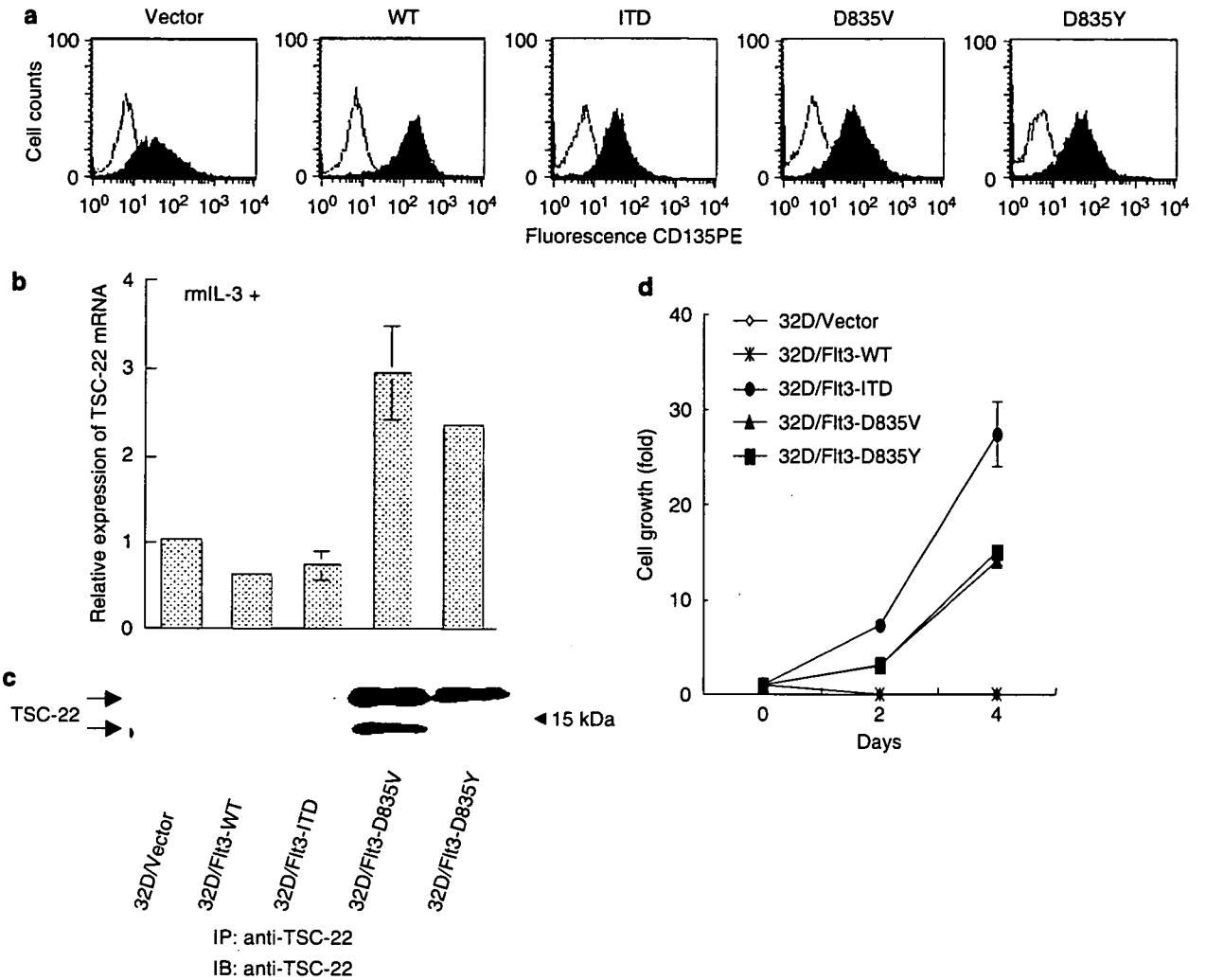

Figure 2 TSC-22 was upregulated by Flt3-TKD, but not by Flt3-ITD. (**a**) Surface expression of transduced Flt3 receptors. 32D cells infected with vector control, Flt3-WT, Flt3-ITD, Flt3-D835V and Flt3-D835Y viruses were stained with isotype control mAb (blank areas) and anti-PE-conjugated CD135 mAb (filled areas). (**b**) Quantification of TSC-22 mRNA levels in 32D cells by real-time RT-PCR. Total RNA was isolated from 32D transfectants cultured as indicated. The bar represents the ratios of GAPDH-normalized expression values. The mean of the expression levels in vector-plasmid transfected cells was set as 1. Each bar represents the mean of three independent experiments. (**c**) The expression levels of TSC-22 protein in 32D transfectants. Equivalent amounts of cell extracts prepared from 32D transfectants were immunoprecipitated with anti-TSC-22 antibody, followed by immunoblotting with the same antibody. (**d**) The growth of 32D transfectants. 32D cells infected with Vector, Flt3-WT, Flt3-ITD, Flt3-D835V or Flt3-D835Y viruses were seeded at a density of 1×10^4 cell/ml on 96-well plates in the absence of growth factor. Viable cells of triplicate cultures were quantitated by measuring luminescence using a Micro Lumat Plus luminometer at the indicated times. The means and s.d. are shown. GAPDH, glyceraldehyde-3-phosphate dehydrogenase; mAb, monoclonal antibody; PE, phycoerythrin; RT-PCR, reverse transcription-PCR; TSC-22, TGF-β-stimulated clone-22.

proliferation of leukemic cells, we injected Flt3-ITD-transduced 32D cells with or without enforced expression of TSC-22 into the C3H/HeJ mice. Overexpression of TSC-22 marginally extended the survival of C3H/HeJ mice inoculated with Flt3-ITD-transduced 32D cells (Figure 3f), suggesting attenuated growth of the leukemic cells by TSC-22. We concluded that enforced expression of TSC-22 led to decreased growth rates in several leukemia-derived cell lines.

32D cells acquire adhesive properties by forced expression of TSC-22

A differentiation block is one of the characteristics of leukemia cells. As previously reported by Zheng *et al.*,[45] 32D cells differentiated into mature granulocytes in the presence of G-CSF, while Flt3-ITD-expressing 32D cells did not. To examine whether TSC-22 was involved in the differentiation, we performed a similar experiment using Flt3-ITD-carrying 32D cells transfected with the TSC-22 construct. Forced expression of TSC-22 did not affect the differentiation into granulocytes in the presence or absence of G-CSF (data not shown). However, we found that parental or Flt3-ITD-carrying 32D cells adhered to the plastic plates by forced expression of TSC-22. To confirm this, an adhesion assay using BSA- or FB-coated plates was conducted. As shown in Figure 4a, the number of cells adhering to the plates was significantly increased by forced expression of TSC-22. The adherent cells displayed well-spread morphology, similar to monocytes/macrophages (Figure 4b). Expression levels of several integrins and surface markers indicative of granulocytes or monocytes/macrophages did not change except that CD11b expression level was slightly increased by the enforced expression of TSC-22 (data not shown). These results indicated that TSC-22 might play a role in the differentiation, giving an adhesive property to the cells.

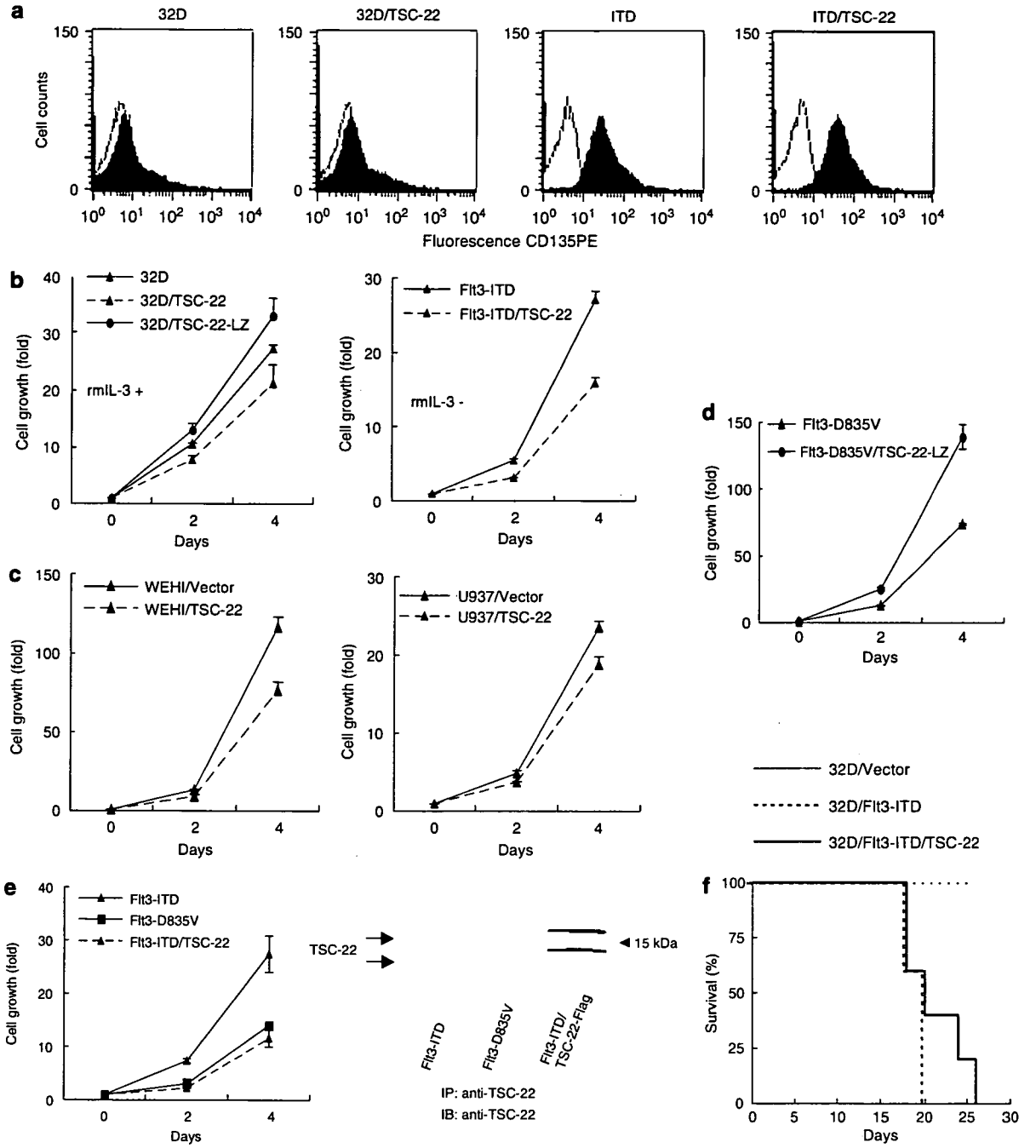

Figure 3 Forced expression of TSC-22 suppressed the proliferation of 32D, WEHI and U937 cells. (**a**) Surface expression of endogenous Flt3 and transduced Flt3-ITD. 32D or Flt3-ITD-transduced 32D cells were infected with TSC-22 or vector control viruses and stained with isotype control mAb (blank areas) and anti-PE-conjugated CD135 mAb (filled areas). (**b–d**) The growth of several cell transfectants. 32D, Flt3-ITD-transduced 32D cells infected with TSC-22, TSC-22-LZ or vector control viruses (**b**), WEHI, U937 cells infected with TSC-22 or empty vectors (**c**), and Flt3-D835V-transduced 32D cells infected with TSC-22-LZ or vector control viruses (**d**) were seeded at a density of 1×10^4 cell/ml into 96-well plates with or without growth factor. Viable cells of triplicate cultures were quantitated as described previously at the indicated times. The means and s.d. are shown. (**e**) Growth rates of the Flt3 transfectants. Flt3-ITD-, Flt3-D835V-transduced 32D cells and Flt3-ITD-expressing 32D cells co-transduced with TSC-22 were examined (left panel). Expression levels of endogenous and exogenous TSC-22 among these cells were determined as described above (right panel). (**f**) Kaplan–Meier plot of survival. C3H/HeJ mice ($n = 5$ in each group) were injected via tail vein with 1×10^5 of 32D cells expressing Flt3-ITD, Flt3-ITD/TSC-22 and vector as control. Mouse survival was monitored daily. The percentage of surviving mice (y axis) is plotted over the time after injection (x axis). This graph presents data from two independent experiments. mAb, monoclonal antibody; PE, phycoerythrin; TSC-22, TGF-β-stimulated clone-22.

Expression of TSC-22 promotes monocytic differentiation of several leukemia cells

To elucidate the role of TSC-22 in the differentiation of leukemia cells, we performed experiments using differentiation-inducing reagents. When U937 cells transfected with a TSC-22 construct or vector alone were exposed to 10 ng/ml PMA, both TSC-22-transduced and control U937 cells showed decreased proliferation. However, TSC-22-carrying U937 cells treated with PMA

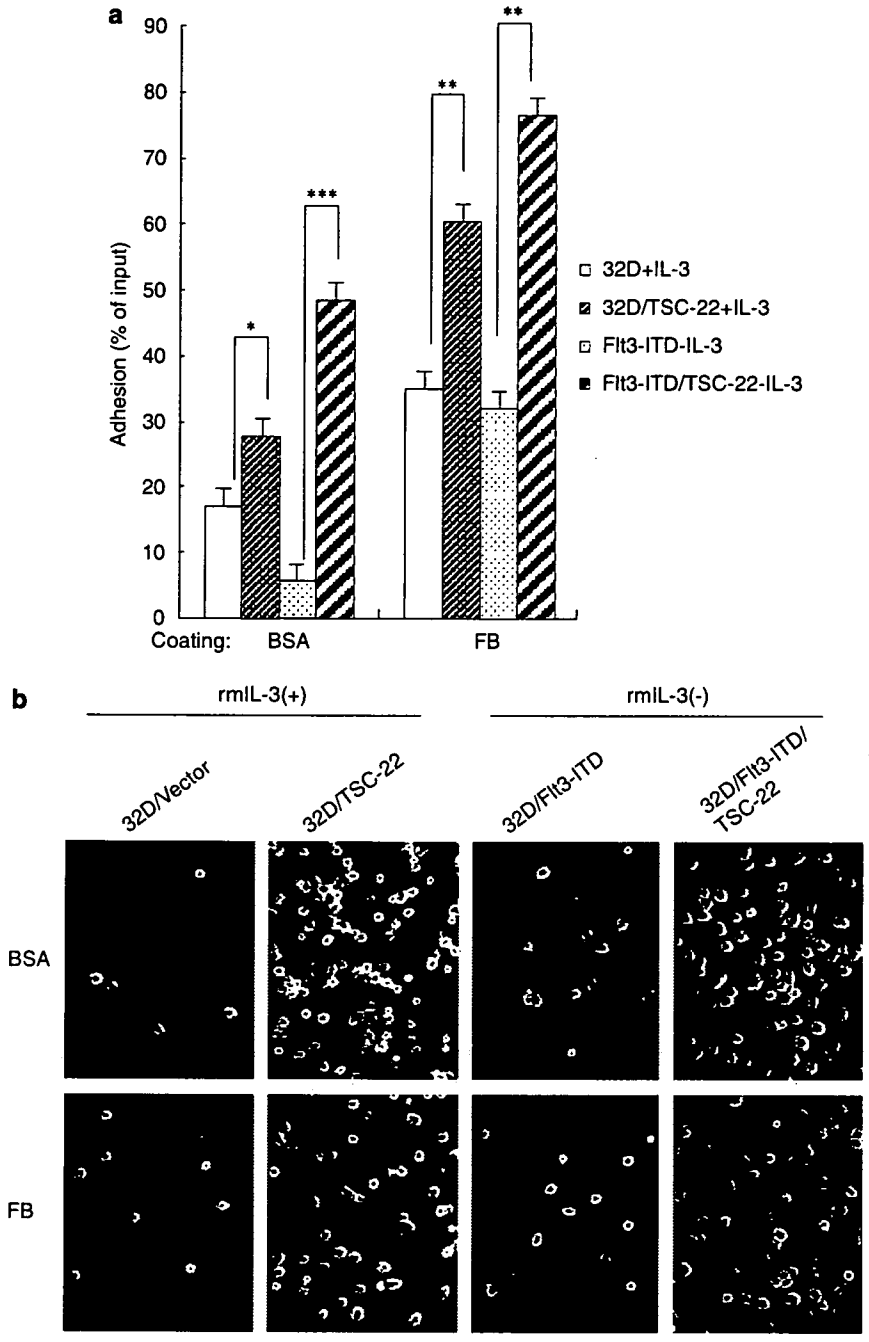

Figure 4 Forced expression of TSC-22 induced adhesion of 32D cells to BSA and FB. 32D and Flt3-ITD-transduced 32D cells infected TSC-22 or vector control viruses were seeded at a density of 2×10^5 cell/ml on 96-well plates coated with BSA or FB for 2 h at 37°C. After washing three times, the percentage of adherent cells was analyzed by Micro Lumat Plus luminometer (**a**) or by microscope (× 100) (**b**). The statistical significance of differences between transduced cells and control cells is indicated by asterisks, ***$P<0.001$, **$P<0.01$, *$P<0.05$. BSA, bovine serum albumin; FB, Fibrinogen.

showed stronger growth arrest as compared with U937 control cells (Figure 5a). Morphological analysis showed that TSC-22-transduced U937 cells treated with PMA differentiated more efficiently into mature monocytes, the characteristic phenotypes of which were cell spreading, reduced nucleus-to-cytoplasm ratios and appearance of vacuoles (Figure 5b). In accordance with morphological changes, flow cytometry analysis demonstrated that the mean fluorescence intensity (MFI) of CD11b, CD14, CD80 and HLA-DR dramatically increased in TSC-22-expressing U937 cells compared to control U937 cells after PMA treatment, suggesting that differentiation into mature monocytes was efficiently induced in TSC-22-transduced U937 cells (Figure 5c). We also observed similar effects of TSC-22 on Vit.D3-induced differentiation of U937 (Figure 5c).

To further confirm the effect of TSC-22 on the monocytic differentiation of leukemia cells, another human leukemia cell line HL-60 was utilized. As was the case for U937 cells, fluorescence-activated cell sorting analysis showed that higher MFI of CD11b was observed in TSC-22-transduced HL-60 cells as compared with control HL-60 cells in response to either PMA or Vit.D3 (Figure 5d). Collectively, these data suggested that forced expression of TSC-22 played a role in monocytic

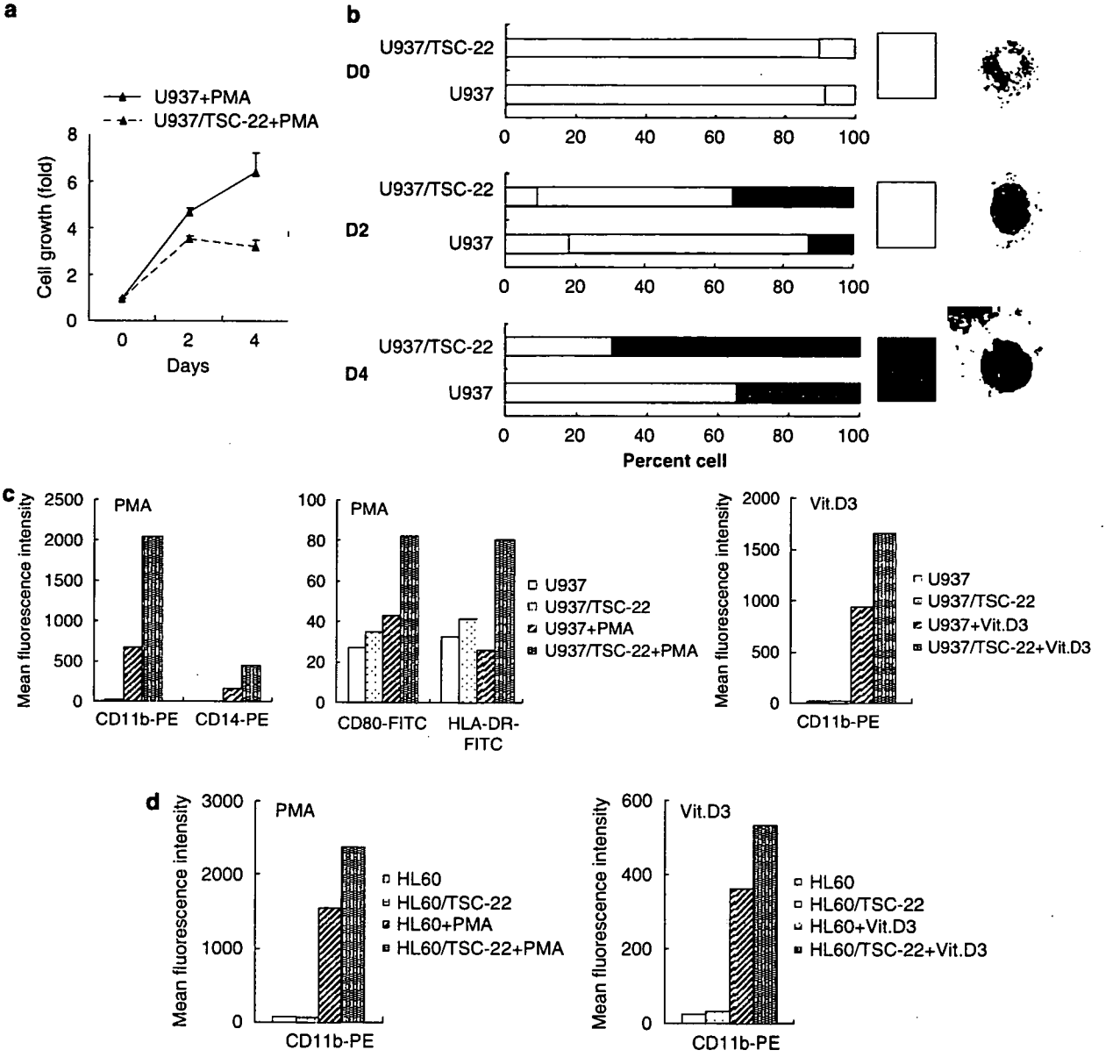

Figure 5 Forced expression of TSC-22 promoted PMA- and Vit.D3-induced monocytic differentiation of human leukemia cell lines. (**a**) Growth inhibition of U937 transfectants with PMA treatment. U937 transfectants were treated with PMA and viable cells of triplicate cultures were quantitated as described previously. (**b**) Differentiation of U937 transfectants with PMA treatment. TSC-22-transduced or control U937 cells were treated with PMA. After 2 or 4 days, cells were stained with May-Grunwald-Giemsa and morphologically analyzed by light microscopy. Cells were grouped into three categories: undifferentiated cells, moderately differentiated cells and terminally differentiated cells. Each photograph on the right column shows typical findings. The percentage of PMA-treated cells under each differentiation stage is shown. (**c**) Surface expression of monocytic markers on U937 transfectants. TSC-22-transduced or control U937 cells were stimulated with PMA or Vit.D3 for 48 h. The surface expression of CD11b, CD14, CD80 and HLA-DR in the cells was evaluated in terms of MFI by flow cytometer. (**d**) Surface expression of monocytic markers on HL-60 transfectants. TSC-22-transduced or control HL-60 cells were stimulated with PMA or Vit.D3 for 48 h. The surface expression of CD11b was evaluated by flow cytometer. HLA-DR, human leukocyte antigen-DR; MFI, mean fluorescence intensity; TSC-22, TGF-β-stimulated clone-22.

differentiation of several leukemia cells. Therefore, TSC-22 appears to have the potential to suppress the growth of several leukemia cells, in part by promoting differentiation into monocytes.

Discussion

Leukemia is caused by multiple gene alterations, including chromosomal translocations, deletions and point mutations. Among them, constitutive activation of a tyrosine kinase receptor Flt3 is the most common mutation found in 30–40% of patients with AML as well as in some patients with myelodysplastic syndromes. There are two types of Flt3 mutations, Flt3-ITD and Flt3-TKD. Overexpression of the WT Flt3 frequently associated with autonomous expression of Flt3 ligand is also found in leukemic patients. These facts indicate that Flt3 activation is pivotal in leukemogenesis in a large population of patients with AML. Both Flt3-ITD and Flt3-TKD constitutively stimulate the downstream signaling pathways;

however, only Flt3-ITD was found to be associated with poor prognosis.[8,12,13,16,20–23]

In the present study, we confirmed that Flt3-ITD was more potent than Flt3-D835V in inducing cell transformation by *in vivo* experiments where Ba/F3 cells expressing Flt3-ITD or Flt3-D835V were transplanted into syngeneic recipient mice. To clarify why Flt3-ITD is more oncogenic than Flt3-TKD, we compared the gene expression profiles of Ba/F3 cells expressing Flt3-ITD and Flt3-D835V. Among the genes upregulated or downregulated by Flt3-D835V as compared with Flt3-ITD, we focused on one of the upregulated genes, TSC-22, a potential tumor suppressor originally identified as a TGF-β-induced gene. Indeed, experiments using an Flt3 inhibitor and Flt3 siRNA confirmed that both expression and kinase activity of Flt3-TKD are required for upregulation of TSC-22. Several studies demonstrated that high expression of TSC-22 inhibited the growth or induced the differentiation of a variety of human tumor cell lines, such as gastric carcinoma cells,[36] breast cancer cells,[32] salivary gland cancer cells,[29,37,38] brain tumors[46] and prostate cancer cells.[47] The findings that anticancer drugs increased or carcinogens decreased the expression of TSC-22 support the concept that TSC-22 can be a key molecule in cancer therapy. TSC-22 expression was also enhanced by various cytokines and growth factors.[26–33] Further study is now under way to determine in which part of signaling pathways TSC-22 integrates. TSC-22 mRNA is expressed in various hematopoietic cell lines as well as bone marrow-derived cells, including macrophages, mast cells and dendritic cells (data not shown). While TSC-22 expression significantly inhibited the growth of several cell lines, including 32D, WEHI and U937, it profoundly inhibited the growth of Flt3-ITD-transduced 32D cells (Figure 3b). Expression of TSC-22 in Ba/F3 cells only weakly inhibited the growth and did not significantly improve the prognosis of Balb/c mice inoculated with Flt3-ITD-transduced Ba/F3 cells (data not shown). This is probably because the endogenous expression level of TSC-22 in Ba/F3 cells is much higher than those in other cell lines (data not shown). Therefore, we used 32D cells in both *in vitro* and *in vivo* experiments that express much less amount of TSC-22. A dominant-negative form of TSC-22 accelerated the growth of 32D cells, which is consistent with the growth suppressive effects of TSC-22 on leukemic cells. In addition, expression of TSC-22 in Flt3-ITD-transduced 32D cells seemed to improve the prognosis of C3H/HeJ mice inoculated with Flt3-ITD-transduced 32D cells. Thus, although we still do not know if the difference in clinical outcomes is relevant to the differing expression levels of TSC-22 downstream of Flt3-ITD and Flt3-TKD, the increased expression of TSC-22 may explain at least in part the attenuated growth of Flt3-TKD-expressing cells when compared to Flt3-ITD-expressing cells. According to recent reports, activation of STAT5, mitogen-activated protein kinase (MAPK) and protein kinase B(Akt) and repression of the myeloid transcription factors CCAAT/enhancer binding protein α (EβPα) and PU.1 are relevant to potent transforming abilities of Flt3-ITD-bearing cells.[18,24,25,48] However the activation of STAT5, MAPK and Akt was not affected by enforced expression of TSC-22 (data not shown), suggesting that TSC-22 is rather downstream but not upstream of these signaling molecules. Further investigation is required where and how TSC-22 integrates in the signal transduction pathway. To fully evaluate the impact of TSC-22 on leukemogenesis, experiments involving bone marrow transplantation using TSC-22 knock out mice will be useful.

In general, the suppression of growth is associated with the induction of apoptosis or cell-cycle arrest. In fact, TSC-22 induces the apoptosis of several cancer cells, as reported by Ohta *et al.*[36] and Uchida *et al.*[49] However, neither apoptosis nor cell-cycle arrest was significantly induced in TSC-22-transduced leukemia cells (data not shown). Instead, we found that monocytic differentiation of several leukemia cells was accelerated by the forced expression of TSC-22. This effect was more evident when differentiation-inducing reagents were given (Figures 5c and d). On the other hand, G-CSF-induced granulocytic differentiation of 32D cells was not enhanced by TSC-22 expression.

A differentiation block is one of the two major causes of leukemogenesis, acting in concert with progressive proliferation or inhibition of apoptosis. Thus, TSC-22 may exert growth-suppressive effects on leukemia cells in part through the acceleration of monocytic differentiation. Although Choi *et al.*[50] reported that TSC-22-induced erythroid differentiation of K562 cells by enhancing TGF-β signaling, the differentiation was not induced by cooperation with TGF-β signaling in the TSC-22-transduced leukemia cells we used. In acute promyelocytic leukemia (APL), all-*trans* retinoic acid (ATRA) is a potent inducer of differentiation in APL cells. Moreover, combinatorial use of ATRA and G/granulocyte macrophage-CSF promoted myelomonocytic differentiation, as reported by Glasow *et al.*[51] Our data, together with recent findings, suggest that combination of chemical compounds that increase TSC-22 expression and differentiation-inducing drugs will be attractive as a new therapy for leukemia. TSC-22 is considered to be a transcriptional regulator because of its leucine zipper-like structure; however, the precise mechanism by which TSC-22 functions in the differentiation of leukemia cells remains to be elucidated.

In conclusion, the increased expression of TSC-22 downstream of Flt3-D835V was not observed downstream of Flt3-ITD. Forced expression of TSC-22 suppresses the growth and promotes the monocytic differentiation of several leukemia cells, in particular, in combination with differentiation-inducing reagents. TSC-22 appears promising in developing more effective therapy for leukemia.

Acknowledgements

We thank Dr Hitoshi Kawamata for providing plasmid pEGFP-TSC-22-LZ. We thank Dr Naoko Watanabe, Dr Yoshinori Yamanishi, Dr Kumi Izawa and Dr Yukinori Minoshima for valuable discussions, Fumi Shibata, Miyuki Ito and Ai Hishiya for excellent technical assistance. We also thank R&D Systems for cytokines. This work was supported in part by Grants-in-Aid from the Ministry of Education, Science, Technology, Sports, and Culture in Japan.

References

1 Matthews W, Jordan CT, Wiegand GW, Pardoll D, Lemischka IR. A receptor tyrosine kinase specific to hematopoietic stem and progenitor cell-enriched populations. *Cell* 1991; **65**: 1143–1152.
2 Rosnet O, Marchetto S, deLapeyriere O, Birnbaum D. *Oncogene* 1991; **6**: 1641–1650.
3 Small D, Levenstein M, Kim E, Carow C, Amin S, Rockwell P *et al.* STK-1, the human homolog of Flk-2/Flt3, is selectively expressed in CD34+ human bone marrow cells and is involved in the proliferation of early progenitor/stem cells. *Proc Natl Acad Sci USA* 1994; **91**: 459–463.
4 Rosnet O, Buhring HJ, Marchetto S, Rappold I, Lavagna C, Sainty D *et al.* Human FLT3/FLK2 receptor tyrosine kinase is expressed at the surface of normal and malignant hematopoietic cells. *Leukemia* 1996; **10**: 238–248.
5 Mackarehtschian K, Hardin JD, Moore KA, Boast S, Goff SP, Lemischka IR. Targeted disruption of the flk2/flt3 gene leads to

deficiencies in primitive hematopoietic progenitors. *Immunity* 1995; **3**: 147–161.
6 Birg F, Courcoul M, Rosnet O, Bardin F, Pebusque MJ, Marchetto S *et al.* Expression of the FMS/KIT-like gene FLT3 in human acute leukemias of the myeloid and lymphoid lineages. *Blood* 1992; **80**: 2584–2593.
7 Carow CE, Levenstein M, Kaufmann SH, Chen J, Amin S, Rockwell P *et al.* Expression of the hematopoietic growth factor receptor FLT3 (STK-1/Flk2) in human leukemias. *Blood* 1996; **87**: 1089–1096.
8 Nakao M, Yokota S, Iwai T, Kaneko H, Horiike S, Kashima K *et al.* Internal tandem duplication of the Flt3 gene found in acute myeloid leukemia. *Leukemia* 1996; **10**: 1911–1918.
9 Kiyoi H, Towatari M, Yokota S, Hamaguchi M, Ohno R, Saito H *et al.* Internal tandem duplication of the FLT3 gene is a novel modality of elongation mutation which causes constitutive activation of the product. *Leukemia* 1998; **12**: 1333–1337.
10 Meshinchi S, Woods WG, Stirewalt DL, Sweetser DA, Buckley JD, Tjoa TK *et al.* Prevalence and prognostic significance of Flt3 internal tandem duplication in pediatric acute myeloid leukemia. *Blood* 2001; **97**: 89–94.
11 Stirewalt DL, Kopecky KJ, Meshinchi S, Appelbaum FR, Slovak ML, Willman CL *et al.* FLT3, RAS and TP53 mutations in elderly patients with acute myeloid leukemia. *Blood* 2001; **97**: 3589–3595.
12 Schnittger S, Schoch C, Dugas M, Kern W, Staib P, Wuchter C *et al.* Analysis of FLT3 length mutations in 1003 patients with acute myeloid leukemia: correlation to cytogenetics, FAB subtype, and prognosis in the AMLCG study and usefulness as a marker for the detection of minimal residual disease. *Blood* 2002; **100**: 59–66.
13 Thiede C, Steudel C, Mohr B, Schaich M, Schakel U, Platzbecker U *et al.* Analysis of FLT3-activating mutations in 979 patients with acute myelogenous leukemia: association with FAB subtypes and identification of subgroups with poor prognosis. *Blood* 2002; **99**: 4326–4335.
14 Yamamoto Y, Kiyoi H, Nakano Y, Suzuki R, Kodera Y, Miyawaki S *et al.* Activating mutation of D835 within the activation loop of FLT3 in human hematologic malignancies. *Blood* 2001; **97**: 2434–2439.
15 Abu-Duhier FM, Goodeve AC, Wilson GA, Care RS, Peake IR, Reilly JT. Identification of novel FLT3 Asp835 mutations in adult acute myeloid leukaemia. *Br J Haematol* 2001; **113**: 983–988.
16 Kottaridis PD, Gale RE, Frew ME, Harrison G, Langabeer SE, Belton AA *et al.* The presence of a FLT3 internal tandem duplication in pa-tients with acute myeloid leukemia (AML) addsimportant prognostic information to cytogeneticrisk group and response to the first cycle of che-motherapy: analysis of 854 patients from theUnited Kingdom Medical Research Council AML10 and 12 trials. *Blood* 2001; **98**: 1752–1759.
17 Hayakawa F, Towatari M, Kiyoi H, Tanimoto M, Kitamura T, Saito H *et al.* Tandem-duplicated Flt3 constitutively activates STAT5 and MAP kinase and introduces autonomous cell growth in IL-3-dependent cell lines. *Oncogene* 2000; **19**: 624–631.
18 Mizuki M, Fenski R, Halfter H, Matsumura I, Schmidt R, Muller C *et al.* Flt3 mutations from patients with acute myeloid leukemia induce transformation of 32D cells mediated by the Ras and STAT5 pathways. *Blood* 2000; **96**: 3907–3914.
19 Fenski R, Flesch K, Serve S, Mizuki M, Oelmann E, Kratz-Albers K *et al.* Constitutive activation of FLT3 in acute myeloid leukaemia and its consequences for growth of 32D cells. *Br J Haematol* 2000; **108**: 322–330.
20 Stirewalt DL, Radich JP. The role of FLT3 in haematopoietic malignancies. *Nat Rev Cancer* 2003; **3**: 650–665.
21 Shih LY, Huang CF, Wu JH, Lin TL, Dunn P, Wang PN *et al.* Internal tandem duplication of FLT3 in relapsed acute myeloid leukemia: a comparative analysis of bone marrow samples from 108 adult patients at diagnosis and relapse. *Blood* 2002; **100**: 2387–2392.
22 Moreno I, Martin G, Bolufer P, Barragan E, Rueda E, Roman J *et al.* Incidence and prognostic value of FLT3 internal tandem duplication and D835 mutations in acute myeloid leukemia. *Haematologica* 2003; **88**: 19–24.
23 Levis M, Small D. FLT3: ITDoes matter in leukemia. *Leukemia* 2003; **17**: 1738–1752.
24 Spiekermann K, Bagrintseva K, Schwab R, Schmieja K, Hiddemann W. Overexpression and constitutive activation of FLT3 induces STAT5 activation in primary acute myeloid leukemia blast cells. *Clin Cancer Res* 2003; **9**: 2140–2150.
25 Choudhary C, Schwable J, Brandts C, Tickenbrock L, Sargin B, Kindler T *et al.* AML-associated Flt3 kinase domain mutations show signal transduction differences compared with Flt3 ITD mutations. *Blood* 2005; **106**: 265–273.
26 Shibanuma M, Kuroki T, Nose K. Isolation of a gene encoding a putative leucine zipper structure that is induced by transforming growth factor beta 1 and other growth factors. *J Biol Chem* 1992; **267**: 10219–10224.
27 Ohta S, Shimekake Y, Nagata K. Molecular cloning and characterization of a transcription factor for the C-type natriuretic peptide gene promoter. *Eur J Biochem* 1996; **242**: 460–466.
28 Jay P, Ji JW, Marsollier C, Taviaux S, Berge-Lefranc JL, Berta P. Cloning of the human homologue of the TGF beta-stimulated clone 22 gene. *Biochem Biophys Res Commun* 1996; **222**: 821–826.
29 Kawamata H, Nakashiro K, Uchida D, Hino S, Omotehara F, Yoshida H *et al.* Induction of TSC-22 by treatment with a new anti-cancer drug, vesnarinone, in a human salivary gland cancer cell. *Br J Cancer* 1998; **77**: 71–78.
30 Hamil KG, Hall SH. Cloning of rat Sertoli cell follicle-stimulating hormone primary response complementary deoxyribonucleic acid: regulation of TSC-22 gene expression. *Endocrinology* 1994; **134**: 1205–1212.
31 Kawa-uchi T, Nifuji A, Mataga N, Olson EN, Bonaventure J, Shinomiya K *et al.* Fibroblast growth factor downregulates expression of a basic helix-loop-helix-type transcription factor, scleraxis, in a chondrocyte-like cell line, TC6. *J Cell Biochem* 1998; **70**: 468–477.
32 Kester HA, van der Leede BM, van der Saag PT, van der Burg B. Novel progesterone target genes identified by an improved differential display technique suggest that progestin-induced growth inhibition of breast cancer cells coincides with enhancement of differentiation. *J Biol Chem* 1997; **272**: 16637–16643.
33 Trenkle T, Welsh J, Jung B, Mathieu-Daude F, McClelland M. Non-stoichiometric reduced complexity probes for cDNA arrays. *Nucleic Acids Res* 1998; **26**: 3883–3891.
34 Dohrmann CE, Belaoussoff M, Raftery LA. Dynamic expression of TSC-22 at sites of epithelial-mesenchymal interactions during mouse development. *Mech Dev* 1999; **84**: 147–151.
35 Kester HA, Ward-van Oostwaard TM, Goumans MJ, van Rooijen MA, van Der Saag PT, van Der Burg B *et al.* Expression of TGF-beta stimulated clone-22 (TSC-22) in mouse development and TGF-beta signalling. *Dev Dyn* 2000; **218**: 563–572.
36 Ohta S, Yanagihara K, Nagata K. Mechanism of apoptotic cell death of human gastric carcinoma cells mediated by transforming growth factor beta. *Biochem J* 1997; **324**: 777–782.
37 Nakashiro K, Kawamata H, Hino S, Uchida D, Miwa Y, Hamano H *et al.* Down-regulation of TSC-22 (transforming growth factor beta-stimulated clone 22) markedly enhances the growth of a human salivary gland cancer cell line *in vitro* and *in vivo*. *Cancer Res* 1998; **58**: 549–555.
38 Hino S, Kawamata H, Uchida D, Omotehara F, Miwa Y, Begum NM *et al.* Nuclear translocation of TSC-22 (TGF-beta-stimulated clone-22) concomitant with apoptosis: TSC-22 as a putative transcriptional regulator. *Biochem Biophys Res Commun* 2000; **278**: 659–664.
39 Murata K, Kumagai H, Kawashima T, Tamitsu K, Irie M, Nakajima H *et al.* Selective cytotoxic mechanism of GTP-14564, a novel tyrosine kinase inhibitor in leukemia cells expressing a constitutively active Fms-like tyrosine kinase 3 (FLT3). *J Biol Chem* 2003; **278**: 32892–32898.
40 Kitamura T, Koshino Y, Shibata F, Oki T, Nakajima H, Nosaka T *et al.* Retrovirus-mediated gene transfer and expression cloning powerful tools in functional genomics. *Exp Hematol* 2003; **31**: 1007–1014.
41 Oki T, Kitaura J, Eto K, Lu Y, Maeda-Yamamoto M, Inagaki N *et al.* Integrin alphaIIbbeta3 induces the adhesion and activation of mast cells through interaction with fibrinogen. *J Immunol* 2006; **76**: 52–60.
42 Weisberg E, Boulton C, Kelly LM, Manley P, Fabbro D, Meyer T *et al.* Inhibition of mutant FLT3 receptors in leukemia cells by the

small molecule tyrosine kinase inhibitor PKC412. *Cancer Cell* 2002; **1**: 433–443.
43 Walters DK, Stoffregen EP, Heinrich MC, Deininger MW, Druker BJ. RNAi-induced down-regulation of FLT3 expression in AML cell lines increases sensitivity to MLN518. *Blood* 2005; **105**: 2952–2954.
44 Kester HA, Blanchetot C, den Hertog J, van der Saag PT, van der Burg B. Transforming growth factor-beta-stimulated clone-22 is a member of a family of leucine zipper proteins that can homo- and heterodimerize and has transcriptional repressor activity. *J Biol Chem* 1999; **274**: 27439–27447.
45 Zheng R, Friedman AD, Small D. Targeted inhibition of FLT3 overcomes the block to myeloid differentiation in 32Dcl3 cells caused by expression of FLT3/ITD mutations. *Blood* 2002; **100**: 4154–4161.
46 Shostak KO, Dmitrenko VV, Garifulin OM, Rozumenko VD, Khomenko OV, Zozulya YA *et al.* Downregulation of putative tumor suppressor gene TSC-22 in human brain tumors. *J Surg Oncol* 2003; **82**: 57–64.
47 Rentsch CA, Cecchini MG, Schwaninger R, Germann M, Markwalder R, Heller M *et al.* Differential expression of TGF beta-stimulated clone 22 in normal prostate and prostate cancer. *Int J Cancer* 2006; **118**: 899–906.
48 Mizuki M, Schwable J, Steur C, Choudhary C, Agrawal S, Sargin B *et al.* Suppression of myeloid transcription factors and induction of STAT response genes by AML-specific Flt3 mutations. *Blood* 2003; **101**: 3164–3173.
49 Uchida D, Kawamata H, Omotehara F, Miwa Y, Hino S, Begum NM *et al.* Over-expression of TSC-22 (TGF-beta stimulated clone-22) markedly enhances 5-fluorouracil-induced apoptosis in a human salivary gland cancer cell line. *Lab Invest* 2000; **80**: 955–963.
50 Choi SJ, Moon JH, Ahn YW, Ahn JH, Kim DU, Han TH. Tsc-22 enhances TGF-beta signaling by associating with Smad4 and induces erythroid cell differentiation. *Mol Cell Biochem* 2005; **271**: 23–28.
51 Glasow A, Prodromou N, Xu K, von Lindern M, Zelent A. Retinoids and myelomonocytic growth factors cooperatively activate RARA and induce human myeloid leukemia cell differentiation via MAP kinase pathways. *Blood* 2005; **105**: 341–349.

Analysis of mouse LMIR5/CLM-7 as an activating receptor: differential regulation of LMIR5/CLM-7 in mouse versus human cells

Yoshinori Yamanishi,[1] Jiro Kitaura,[1] Kumi Izawa,[1] Takayuki Matsuoka,[1] Toshihiko Oki,[1] Yang Lu,[1] Fumi Shibata,[1] Satoshi Yamazaki,[2] Hidetoshi Kumagai,[1] Hideaki Nakajima,[1] Mari Maeda-Yamamoto,[3] Victor L. J. Tybulewicz,[4] Toshiyuki Takai,[5] and Toshio Kitamura[1]

[1]Division of Cellular Therapy, Advanced Clinical Research Center, Institute of Medical Science, University of Tokyo, Tokyo, Japan; [2]Laboratory of Stem Cell Therapy, Center for Experimental Medicine, Institute of Medical Science, University of Tokyo, Tokyo, Japan; [3]National Institute of Vegetable and Tea Science, National Agriculture Research Organization, Shizuoka, Japan; [4]Division of Immune Cell Biology, National Institute for Medical Research, London, United Kingdom; and [5]Department of Experimental Immunology, Institute of Development, Aging and Cancer, Tohoku University, Sendai, Japan

We have analyzed leukocyte mono-Ig–like receptor 5 (LMIR5) as an activating receptor among paired LMIRs. Mouse LMIR5 (mLMIR5) is expressed in myeloid cells such as mast cells, granulocytes, macrophages, and dendritic cells. Cross-linking of transduced mLMIR5 in bone marrow–derived mast cells (BMMCs) caused activation events, including cytokine production, cell survival, degranulation, and adhesion to the extracellular matrix. mLMIR5 associated with DAP12 and to a lesser extent with DAP10, and mLMIR5-mediated functions of BMMCs were strongly inhibited by DAP12 deficiency. Importantly, cross-linking of endogenous mLMIR5 induced Syk-dependent activation of fetal liver–derived mast cells. Unlike mLMIR5, cross-linking of human LMIR5 (hLMIR5) induced cytokine production of BMMCs even in the absence of both DAP12 and DAP10, suggesting the existence of unidentified adaptors. Interestingly, hLMIR5 possessed a tyrosine residue (Y188) in the cytoplasmic region. Signaling via Y188 phosphorylation played a predominant role in hLMIR5-mediated cytokine production in DAP12-deficient, but not wild-type BMMCs. In addition, experiments using DAP10/DAP12 double-deficient BMMCs suggested the existence of Y188 phoshorylation-dependent and -independent signals from unidentified adaptors. Collectively, although both mouse and human LMIR5 play activatory roles in innate immunity cells, the functions of LMIR5 were differentially regulated in mouse versus human cells. (Blood. 2008;111:688-698)

Introduction

It is widely accepted that mast cells are major effector cells in allergic inflammation through a high-affinity IgE receptor (FcεRI). However, recent advances have delineated the significant roles of mast cells in both innate and adaptive immune responses.[1-4]

To find a novel immune receptor expressed on mast cells, we previously performed a signal sequence trap based on retrovirus-mediated expression screening (SST-REX).[5] In this screening, we isolated a cDNA for a novel immune receptor, leukocyte mono-Ig–like receptor 1 (LMIR1),[6] using cDNA library of bone marrow–derived mast cells (BMMCs). Successively, other members of the LMIR family were cloned by searching for sequences homologous with the Ig-like domain of LMIR1. We and others have demonstrated that LMIR1/CMRF-35–like Ig-like molecule-8 (CLM-8)/myeloid-associated Ig-like receptor-I (MAIR-I)/CD300a and LMIR2/CLM-4/MAIR-II/dendritic cell–derived Ig-like receptor 1 (DIgR1)/CD300d as well as LMIR3/CLM-1 and LMIR4/CLM-5 were a pair of inhibitory and activating, respectively, receptors with high homology in the Ig-like domain.[6-14] LMIR/CLM forms a family of paired receptors mainly expressed in myeloid cells.[6-14] In general, activating receptors do not contain any signaling motifs in the short cytoplasmic tails, but transmit signals by associating with immunoreceptor tyrosine–based activation motif (ITAM) or the related activating motif-bearing molecules via a positively charged residue in the transmembrane domain.[15-19] In the present study, we cloned a cDNA for mouse LMIR5 (mLMIR5)/CLM-7 from a BMMC cDNA library. Analysis of DAP10-, DAP12-, and FcRγ-deficient BMMCs demonstrated the predominant role of DAP12 in the activating functions of mLMIR5.

Structural differences in immune receptors in mouse versus human cells sometimes result in differing immunologic responses. For example, human NKG2D associates only with DAP10. On the other hand, mouse NKG2D has 2 splice variants, where the long isoform (NKG2D-L) associates exclusively with DAP10 and the short isoform (NKG2D-S) associates with both DAP10 and DAP12.[20-23] Interestingly, human LMIR5 (hLMIR5)/CD300b/immune receptor expressed by myeloid cell-3 (IREM-3),[24] but not mLMIR5, contained a putative tyrosine phosphorylation motif (YXN) in its short cytoplasmic tail. The present results indicated that DAP12 plays a primary role in functions of mLMIR5, while both DAP12 and DAP10 play roles in functions of its human counterpart hLMIR5. Consistent with a recent report by Martinez-Barriocanal and Sayos,[24] our results also implicated an unidentified adaptor in the hLMIR5-mediated signaling pathway, which was activated through phosphorylation of the tyrosine in the absence of DAP12. In addition, the experiment using DAP12-deficient and

Submitted April 16, 2007; accepted September 18, 2007. Prepublished online as *Blood* First Edition paper, October 10, 2007; DOI 10.1182/blood-2007-04-085787.

The online version of this article contains a data supplement.

The publication costs of this article were defrayed in part by page charge payment. Therefore, and solely to indicate this fact, this article is hereby marked "advertisement" in accordance with 18 USC section 1734.

DAP10/DAP12 double-deficient BMMCs revealed Y188 phosphorylation–dependent and –independent signals downstream of hLMIR5.

Methods

Cells

Murine cell lines used in this study were as follows: FDC-P1, J774-1, RAW264.7, M1, L-G, 32Dcl3, P815, MC/9, L8057, Ba/F3, WEHI231, A20, EL4, BW5147, and DC2.4. L8057 and DC2.4 were a kind gift from Dr Y. Hirabayashi (National Institute of Health Sciences, Tokyo, Japan) and Dr K. L. Rock (University of Massachusetts Medical School, Worcester, MA), respectively. Peripheral blood (PB) cells, bone marrow (BM) cells, splenocytes, thymocytes, and peritoneal cells derived from C57BL/6 mice (or CBA/J mice) were purified as described.[14] CBA/J mice or C57BL/6J mice (Charles River Laboratories Japan, Yokohama, Japan) were used at 8 to 10 weeks of age for isolation of tissues and cells. All procedures were approved by an institutional review committee. BMMCs or fetal liver mast cells (FLMCs) were generated and cultured as described.[25-27] BM-derived macrophage (BMMΦ), BM-derived myeloid dendritic cells (BMmDCs), and BM-derived plasmacytoid dendritic cells (BMpDCs) were cultured as described.[14] The following mutant mice were used: *DAP10*$^{-/-}$,[20] *DAP12*$^{-/-}$,[28] *FcRγ* $^{-/-}$,[29] and *Syk*$^{+/-}$.[30]

Antibodies and other reagents

Cytokines and anti-mLMIR5 polyclonal antibody (Ab) was obtained from R&D Systems (Minneapolis, MN). Fluorescein isothiocyanate (FITC)–conjugated anti–mouse B220, CD3, CD11b, and Gr-1 mAb were purchased from eBioscience (San Diego, CA). FITC-conjugated anti–mouse IgE, FITC-conjugated anti–mouse Ig polyclonal Ab, R-phycoerythrin (PE)–conjugated anti–mouse c-Kit mAb, and mouse antitrinitrophenyl (TNP) IgE (C38-2) were from BD Pharmingen (San Diego, CA). Anti–Flag mAb (M2), mouse IgG1 mAb (MOPC21), goat IgG polyclonal Ab, and mouse antidinitrophenyl (DNP) IgE mAb (SPE-7) were from Sigma-Aldrich (St Louis, MO). Donkey PE-conjugated F(ab')$_2$ anti–goat IgG Ab was from Jackson Immunoresearch Laboratories (West Grove, PA). Anti-Myc mAb (9E10) was from Roche Diagnostics (Indianapolis, IN). Rabbit anti–mouse DAP12 polyclonal Ab was a kind gift from Dr N. Aoki (Asahikawa Medical College, Asahikawa, Japan). Mouse antiphosphotyrosine mAb (4G10) was purchased from Upstate Biotechnology (Charlottesville, VA), and other phospho-specific Abs were from Cell Signaling Technology (Beverly, MA). Other Abs were from Santa Cruz Biotechnology (Santa Cruz, CA). Bovine serum fibronectin (FN), human plasma fibrinogen (FB), and N-glycosidase F were purchased from Sigma-Aldrich, Chemicon (Temecula, CA), and New England Biolabs (Beverly, MA), respectively.

Gene expression analysis

Expression of mLMIR5 was analyzed by reverse transcriptase–polymerase chain reaction (RT-PCR) as described.[14] Amplification of mLMIR5 as well as β-actin for normalization was performed with the following primers: 5′-TTACCATGGAGATGCTCAGG-3 (base: 266-285) and 5′-TCGCTACAGAGAGTGTGTCTCC-3′ (base: 590-569) for mLMIR5; and 5′-CATCACTATTGGCAACGAGC-3′ and 5′-ACGCAGCTCAGTAACAGTCC-3′ for β-actin. Relative expression levels of DAP10, DAP12, and FcRγ among samples were measured by real-time RT-PCR. cDNA was amplified using a LightCycler FastStart DNA Master SYBR Green I kit (Roche Diagnostics, Mannheim, Germany) under the following conditions: 1 cycle of 95°C for 10 seconds, 40 cycles of 95°C for 5 seconds, and 60°C for 20 seconds. All samples were independently analyzed 3 times. The following primers were used: 5′-CCCCCCAGGCTACCTCC-3′ and 5′-TGACATGACCGCATCTGCA-3′ for DAP10; 5′-CAAGATGCGACTGTTCTTCCG-3′ and 5′-GGTCTCTGACCCTGAAGCTCC-3′ for DAP12; 5′-GCCGTGATCTTGTTCTTGCTC-3′ and 5′-CTGCCTTTCGGACCTGGAT-3′ for FcRγ; and 5′-ATGTGTCCGTCGTGGATCTGA-3′ and 5′-TTGAAGTCGCAGGAGACAACC-3′ for GAPDH. Relative gene expression levels were calculated using standard curves generated by serial dilutions of cDNA and normalized by a GAPDH expression level. Product quality was checked by melting curve analysis via LightCycler software (Roche Diagnostics).

DNA constructs

The GenBank/European Molecular Biology Laboratory (EMBL[31])/DNA Data Bank of Japan (DDBJ[32]) database was searched by using the amino acid sequence of the Ig-like domain of mLMIR1. Based on the sequence data, cDNA of mouse and human LMIR5 were isolated by PCR from a cDNA library of BMMCs (derived from CBA/J or B57BL/6 mice) and a cDNA library of human peripheral mononuclear cells (PMCs), respectively, and confirmed by sequencing as described.[6] The cDNA fragment of mLMIR5 or hLMIR5, lacking the signal sequence, was tagged with an Flag or Myc epitope at the N terminus. The resultant Flag or Myc-mLMIR5 or hLMIR5 was subcloned into a pME18s vector containing a SLAM signal sequence (a gift from Hisashi Arase, Osaka University, Osaka, Japan)[33] to generate pME-Flag, Myc-mLMIR5, or hLMIR5. The resultant SLAM signal sequence-Flag, Myc-mLMIR5, or hLMIR5 was subcloned into a pMXs-IRES-puro^r (pMXs-IP)[34] retroviral vector to generate pMXs-Flag or Myc-mLMIR5 or hLMIR5-IP. Two-step PCR mutagenesis was performed in the replacement of K158 (lysine with a positive charge) of hLMIR5 with Q (glutamine with a neutral charge) and Y188 of hLMIR5 with F (phenylalanine).

Transfection and infection

Retroviral transfection was as described.[6,34] Briefly, retroviruses were generated by transient transfection of PLAT-E packaging cells[35] with FuGENE 6 (Roche Diagnostics). BM cells, BMMCs, or Ba/F3 cells were infected with retroviruses in the presence of 10 μg/mL polybrene. After 48 hours, cell selection was started with appropriate antibiotics.[34]

Flow cytometry

Cells were stained as described.[14] Flow cytometric analysis was performed with FACSCalibur (BD Biosciences, Mountain View, CA) equipped with CellQuest software and FlowJo software (Tree Star, Ashland, OR). For mLMIR5 staining, cells were incubated with 20 μg/mL anti-mLMIR5 polyclonal Ab or goat polyclonal IgG Ab as control, before incubation with 10 μg/mL PE-conjugated anti-goat IgG F(ab')$_2$ Ab.

Immunoprecipitation and Western blotting

Cells were lysed with NP-40 lysis buffer containing protease and phosphatase inhibitor cocktail (Sigma-Aldrich). Cell lysates were assayed using a protein assay kit (Bio-Rad, Hercules, CA). Immunoprecipitation and Western blotting were performed as described.[14]

Measurement of cytokines and histamines and adhesion assay

BMMCs and FLMCs were stimulated with either 20 μg/mL anti-mLMIR5 Ab, 20 μg/mL control IgG, or 100 nM phorbol-12-myristate13-acetate (PMA). BMMCs transduced with a Flag-tagged hLMIR5 were stimulated with 20 μg/mL anti-Flag mAb or 20 μg/mL control IgG. In some experiments, BMMCs sensitized with 1 μg/mL anti-TNP IgE for 12 hours were stimulated with 100 ng/mL TNP-BSA. TNF-α, IL-6, and MCP-1 concentrations in culture supernatants were measured using enzyme-linked immunosorbent assay (ELISA) kits (BD Pharmingen and R&D Systems). Histamine released during a 50-minute incubation period was measured as described.[25] Adhesion assay was described previously.[26]

Statistical analysis

Data are shown as means plus or minus standard deviation (SD), and statistical significance was determined by the Student *t* test with *P* levels less than .05 as statistically significant.

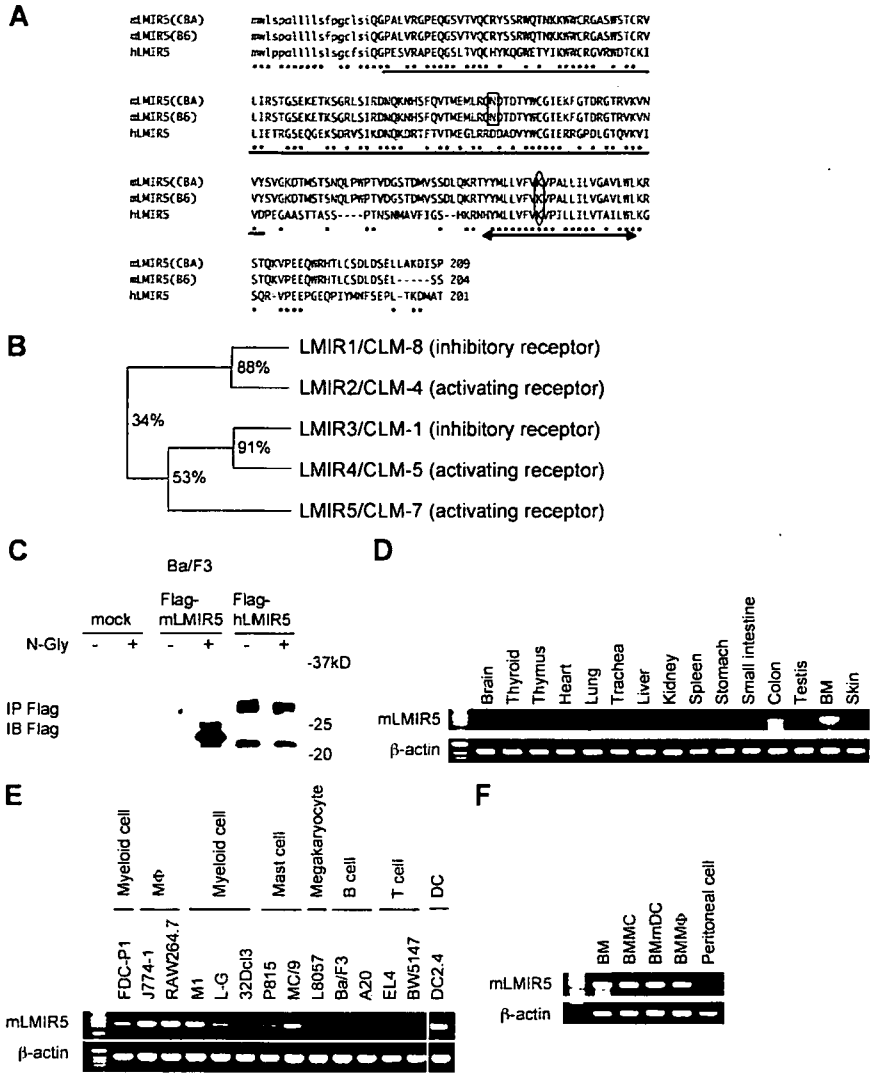

Figure 1. Molecular characteristics and gene expression of LMIR5. (A) Alignment of amino acid sequences for mLMIR5 and hLMIR5. CBA and B6 indicate CBA/J mice and C57BL/6 mice, respectively. *Identical amino acids in mLMIR5 and hLMIR5. The putative signal sequence is shown in lower case. The variable type Ig-like domain is underlined; the potential N-linked glycosylation site is boxed. The transmembrane domain is marked by an arrow; the positive-charged amino acid residue (lysine) in the transmembrane domain is circled. Y188 in the cytoplasmic tail of hLMIR5 is shaded. (B) The phylogenetic tree of LMIR1/2/3/4/5 is shown based on homology with the Ig-like domain. Percentage of identity in amino acid sequences of the Ig-like domain was indicated. (C) Lysates of Ba/F3 cells transduced with either a Flag-tagged mLMIR5, a Flag-tagged hLMIR5, or mock were immnoprecipitated with anti-Flag mAb. The precipitates treated with or without N-glycosidase F were immunoblotted with anti-Flag mAb. (D-F) RT-PCR analysis on mLMIR5 expression in murine tissues (D), hematopoietic cell lines (E), and primary hematopoietic cells (F). Specific primers were used for mLMIR5 or β-actin as control. Vertical lines have been inserted to indicate a repositioned gel lane.

Results

Structure of mLMIR5

To identify other members of LMIR besides LMIR1/2,[6] we searched the database from GenBank/EMBL/DDBJ by using the sequence encoding the Ig-like domain of LMIR1/CLM-8. Based on this, we identified and cloned mLMIR5/CLM-7 in addition to another pair, LMIR3/CLM-1 and LMIR4/CLM-5, from a BMMC cDNA library. An Ig-like domain of mLMIR5 shared 34% and 53% identity at amino acid sequences with that of LMIR1 and LMIR3, respectively (Figure 1A,B).[6] We also cloned its human ortholog from a human PMC cDNA library and found that hLMIR5 shared a 55% identity at overall amino acid sequences with mLMIR5 (Figure 1A). The sequence analysis revealed that mLMIR5 and hLMIR5 are identical to CLM-7[8,9] and IREM-3,[24] respectively. Because hLMIR5/IREM-3 has been recently characterized, we analyzed the structure and functions of mLMIR5/CLM-7 to compare them with those of hLMIR5/IREM-3. mLMIR5 was a type I transmembrane protein composed of an N-terminal signal peptide, an extracellular domain containing a single V-type Ig domain, a transmembrane domain with a positively charged amino acid (lysine), and a short cytoplasmic tail without any signaling motif (Figure 1A). mLMIR5 protein derived from CBA/J mice or B57BL/6 mice was 209 aa or 204 aa, respectively, in length, because the latter was devoid of 5 aa in its cytoplasmic tail. We thereafter used CBA/J mouse–derived LMIR5 as mLMIR5 unless otherwise stated. Interestingly, mLMIR5 does not harbor a putative tyrosine phosphorylation site in the cytoplasmic region (Figure 1A), which is found in hLMIR5.[24]

Next, to examine the characteristics of mLMIR5 at protein levels, we generated Ba/F3 cells expressing either a Flag-tagged mLMIR5 or hLMIR5. Western blot analysis using anti-Flag mAb detected mLMIR5 as a major broad band (26-35 kDa) and a faint band (approximately 24 kDa), while hLMIR5 was detected as a broad band (27-30 kDa) and a discrete band (approximately 22 kDa) (Figure 1C). Treatment with N-glycosidase F diverted the apparent molecular mass of mLMIR5, but not hLMIR5, to several bands ranging from 22 to 26 kDa in size. This was consistent with the presence of a putative N-linked glycosylation site in the extracellular domain of mLMIR5, but not hLMIR5 (Figure 1A,C), suggesting that mLMIR5 was an N-glycoprotein.

mLMIR5 is expressed in myeloid lineage cells

To determine the tissue distribution of mLMIR5, we performed RT-PCR analysis and thereby demonstrated that mLMIR5 was

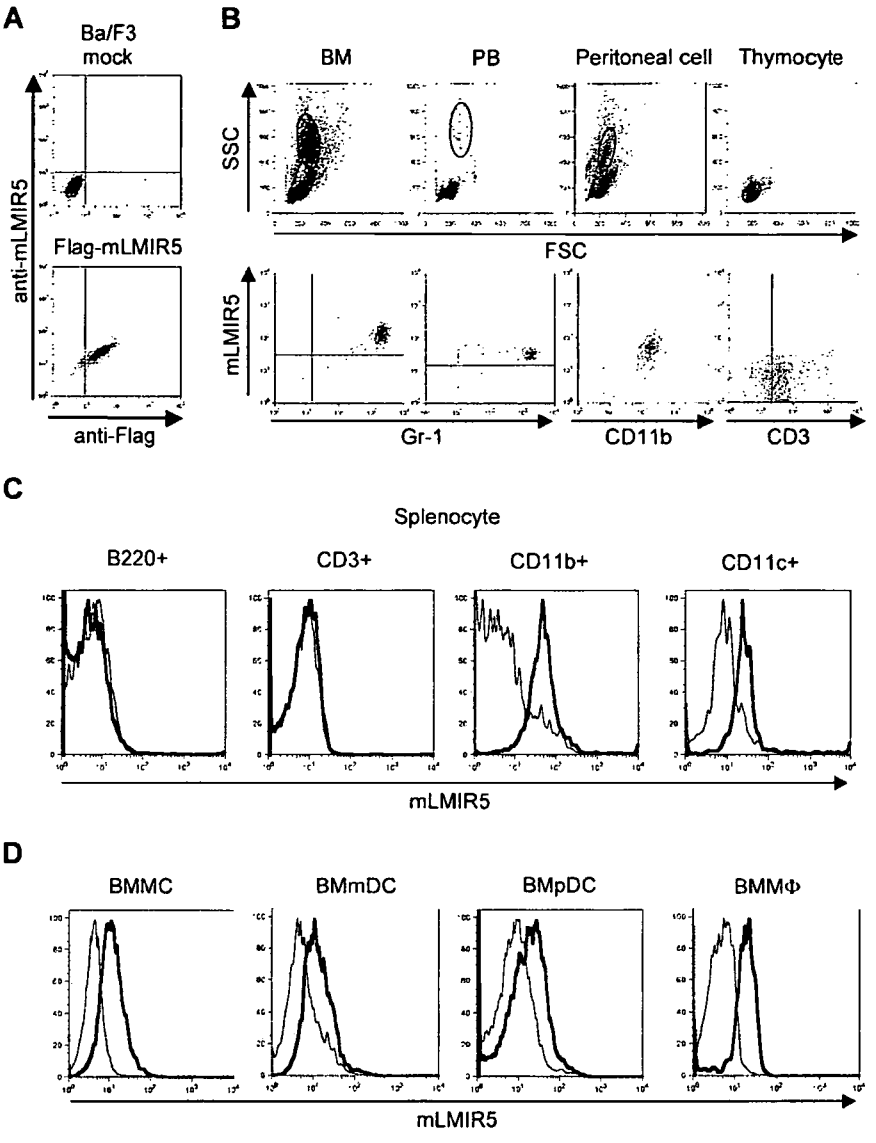

Figure 2. Cell-surface expression of mLMIR5. (A) Ba/F3 cells transduced with a Flag-tagged mLMIR5 or mock were stained with FITC-conjugated mouse IgG1 or anti-Flag Ab as well as polyclonal goat IgG or anti-mLMIR5 Ab, followed by PE-conjugated anti-goat IgG $F(ab')_2$. (B) Analysis of mLMIR5 expression on hematopoietic cells derived from C57BL/6 mice. Single-cell suspensions were prepared from BM, PB, peritoneal cavity, and thymus. Cells were stained with control IgG or anti-mLMIR5 Ab followed by PE-conjugated anti-goat IgG $F(ab')_2$ and FITC-conjugated mAbs as indicated. In BM, PB, and peritoneal cells, $FSC^{high}SSC^{high}$ populations representing myeloid lineage were gated and analyzed for mLMIR5 expression. In thymus, the $FSC^{low}SSC^{low}$ populations representing lymphoid lineage were analyzed. (C) Single-cell suspensions were prepared from spleen. After $B220^+$, $CD3^+$, $CD11b^+$, or $CD11c^+$ cells were sorted by using FITC-conjugated Abs, these cells were stained as described in panel B. (D) Analysis of mLMIR5 expression on murine BM-derived cells. BMMCs, BMmDCs, BMpDCs, and BMMΦ were stained with control IgG or anti-mLMIR5 Ab followed by PE-conjugated anti-goat IgG $F(ab')_2$. The result of control or mLMIR5 staining is shown as a filled or bold-lined histogram, respectively. All the data are representative of 3 independent experiments.

highly expressed in BM and moderately in the lung and colon (Figure 1D). Further investigation of hematopoietic cells revealed that high expression levels of mLMIR5 were observed in myeloid cell lines, including mast, macrophage, and dendritic cell lines, as well as BM-derived cells, but not in T cell lines (Figure 1E,F). Before analyzing surface expression levels of mLMIR5, we confirmed the sensitivity and specificity of polyclonal anti-mLMIR5 Ab, which recognized the extracellular domain of mLMIR5. When Ba/F3 cells were transduced with Flag-tagged mLMIR5, this Ab efficiently detected mLMIR5 on the cell surface, whose expression was confirmed by using anti-Flag mAb (Figure 2A), and anti-mLMIR5 Ab did not detect LMIR1, LMIR2, LMIR3, or LMIR4 transduced into Ba/F3 cells (Figure S1, available on the *Blood* website; see the Supplemental Materials link at the top of the online article). In addition, this polyclonal Ab and anti-Flag Ab gave a similar pattern of several bands in the Western blot of the immunoprecipitates derived from Flag-tagged mLMIR5-transduced Ba/F3 cells. Endogenous mLMIR5 in BMMCs was also detected as a similar pattern. These results confirmed the specificity of this polyclonal Ab raised against mLMIR5 (Figure S3). Surface staining of hematopoietic cell lines with anti-mLMIR5 Ab displayed the results consistent with those from RT-PCR (Figures 1E, S2); A20 cells among the B-cell lines were found to express LMIR5 in both mRNA and protein levels. We then stained a variety of hematopoietic cells using this anti-mLMIR5 Ab. When gated in the population ($FSC^{high}SSC^{high}$), immature granulocytes ($Gr\text{-}1^{high}$) in BM and macrophages ($CD11b^{high}$) in peritoneal cells displayed higher expression levels of mLMIR5, while mature granulocytes ($Gr\text{-}1^{high}$) in PB and dendritic cells ($CD11c^{high}$) in spleen showed detectable but lower expression levels as compared with immature granulocytes. However, neither B cells ($B220^{high}$) in spleen nor T cells ($CD3^{high}$) in spleen and thymus expressed mLMIR5 on their surfaces (Figure 2B,C). In addition, mLMIR5 was expressed in BM-derived cells such as BMMCs, BMmDCs, BMpDCs, and BMMΦ (Figure 2D). LMIR5 expression was also confirmed in several types of mast cells, including peritoneal mast cells and FLMCs (Figure 2D; data not shown). Collectively, mLMIR5 was mainly expressed in myeloid cells.

mLMIR5 associates strongly with DAP12 and to a lesser extent with DAP10 in mLMIR5-transduced cells

The presence of a positively charged residue (lysine) in the transmembrane suggested that LMIR5 associated with adaptor

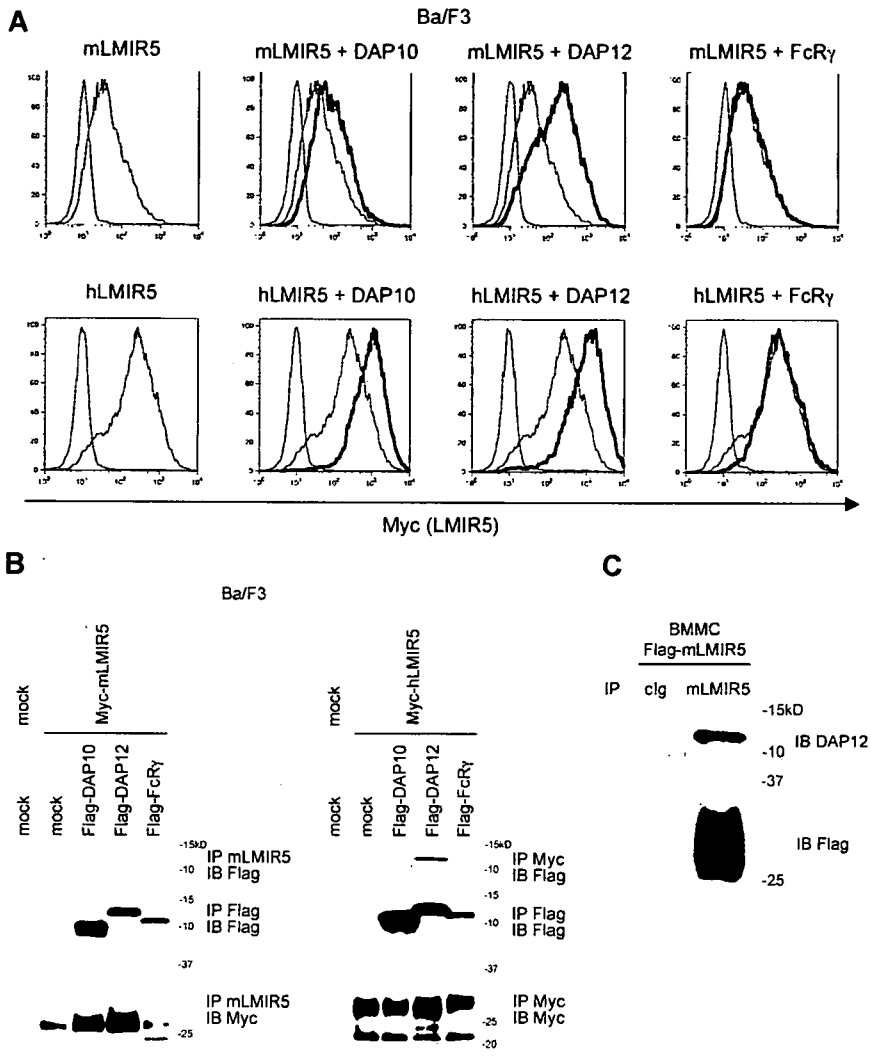

Figure 3. Association of LMIR5 with adaptor molecules such as DAP10, DAP12, and FcRγ. (A,B) Ba/F3 cells were cotransduced with a Myc-tagged mLMIR5 or hLMIR5 and either a Flag-tagged DAP10, DAP12, FcRγ, or mock. (A) Cell-surface expression levels of mLMIR5 (top row) or hLMIR5 (bottom row) were analyzed by flow cytometry by staining cells with control mouse IgG1 or anti-Myc mAb, followed by FITC-conjugated anti-mouse Ig polyclonal Ab. The result of LMIR5 staining in the presence or absence of indicated adaptor molecule was represented by bold- or thin-lined histograms, respectively, while that of control staining was represented by a filled histogram. (B) Lysates of trasduced-Ba/F3 cells were immunoprecipitated with anti-mLMIR5 Ab, anti-Myc Ab, or anti-Flag mAb, and then immunoblotted with anti-Flag mAb or anti-Myc mAb. (C) Lysates of mLMIR5-transduced BMMCs were immnoprecipitated with control IgG or anti-mLMIR5 Ab, and then immunoblotted with anti-DAP12 Ab or anti-Flag mAb.

molecules—such as DAP10, DAP12, and FcRγ—containing a negatively charged residue within the transmembrane domain. To test this, we generated Ba/F3 cells cotransfected with retroviruses expressing a Myc-tagged mLMIR5 or hLMIR5 together with either a Flag-tagged DAP10, DAP12, FcRγ, or mock. Transduction of either mLMIR5 or hLMIR5 did not alter the expression levels of DAP10 and DAP12 mRNA when tested by real-time PCR (data not shown). Staining of these transfectants with anti-Myc mAb revealed that surface expression levels of mLMIR5 were significantly lower than those of hLMIR5 when LMIR5 was expressed alone. Surface expression levels of mLMIR5 were weakly or strongly elevated by DAP10 transduction or DAP12 transduction, respectively, while those of hLMIR5 were elevated by DAP10 as efficiently as by DAP12 (Figure 3A). The transduction of FcRγ did not influence the surface expression levels of mLMIR5 and hLMIR5 (Figure 3A). To confirm the physical association of mLMIR5 with either DAP10 or DAP12, we performed coimmunoprecipitation experiments; DAP12, but not DAP10, was coimmunoprecipitated with mLMIR5 probably because mLMIR5 more strongly associated with DAP12 compared with DAP10. On the other hand, total expression levels of mLMIR5 were elevated by the transduction of either DAP10 or DAP12, suggesting that these adaptors stabilized mLMIR5. When similar experiments were conducted on hLMIR5, both DAP10 and DAP12 were coimmunoprecipitated with hLMIR5 (Figure 3B). Furthermore, coimmunoprecipitation of endogenous DAP12 with transduced mLMIR5 was observed in BMMCs (Figure 3C). In conclusion, mLMIR5 was capable of associating strongly with DAP12 and to a lesser extent with DAP10, at least in mLMIR5-transduced cells.

Cross-linking of mLMIR5 induces the activation of mast cells

Since mLMIR5 was highly expressed in mast cells, we analyzed the activating functions of mLMIR5 in BMMCs. To obtain strong activation, mLMIR was transduced into BMMCs. When mLMIR5 was engaged by anti-mLMIR5 Ab, but not control Ab, in mLMIR5-transduced BMMCs, strong activation of ERK, p38, and Akt was recognized by using phospho-specific Abs, indicating a cellular activation in mast cells stimulated by LMIR5 cross-linking (Figure 4A). Mast cells, when activated by FcεRI aggregation, cause a variety of activation events such as cytokine/chemokine production and degranulation characterized by histamine release.[1,3,25,36-38] Therefore, we performed experiments to examine whether similar activation events were induced by mLMIR5 engagement. In line with cellular activation, mLMIR5-transduced BMMCs stimulated by anti-mLMIR5 Ab, but not control Ab, produced IL-6, TNF-α, and MCP-1 (Figure 4B), and adhered efficiently to fibronectin or fibrinogen (Figure 4C). On the other hand, degranulation or cell

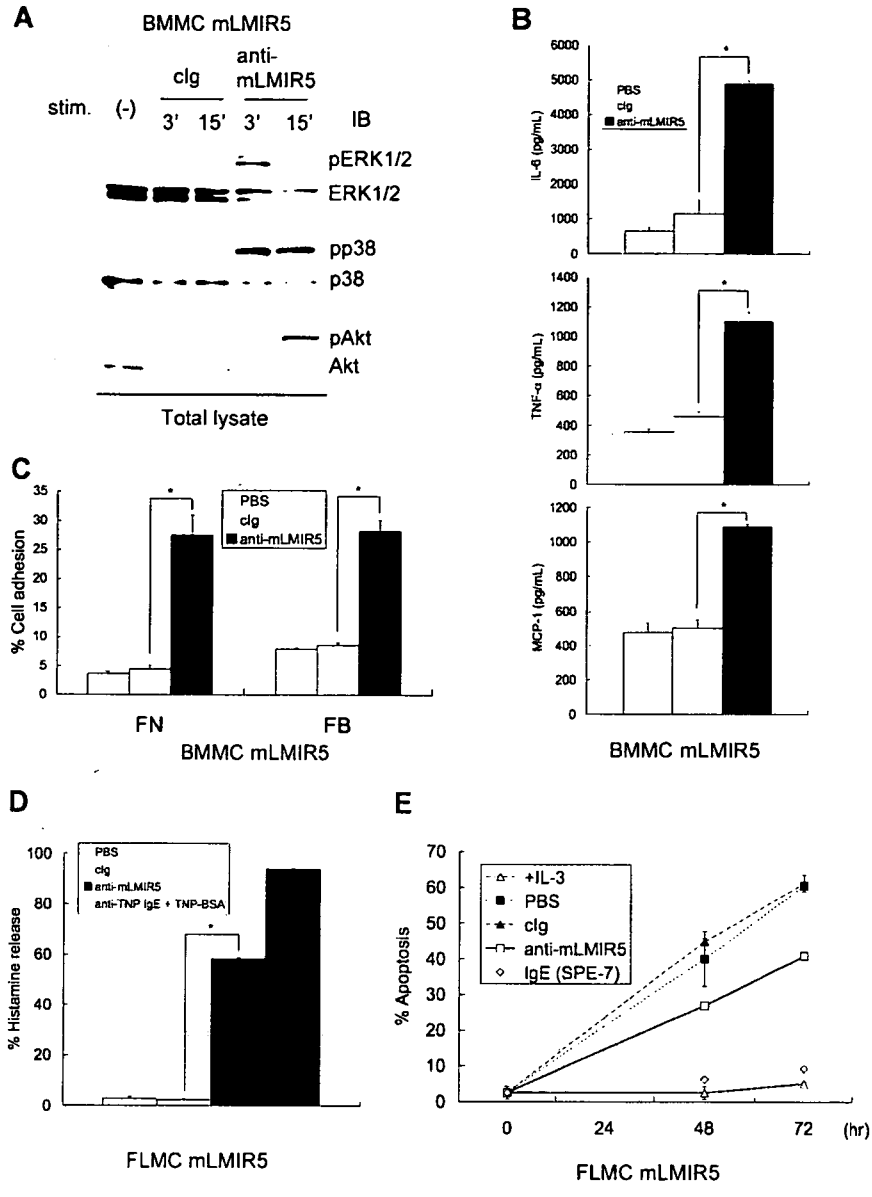

Figure 4. Cross-linking of mLMIR5 induced the phosphorylation of several signaling molecules in mLMIR5-transduced mast cells, resulting in cytokine/chemokine production, cell adhesion, histamine release, and cell survival. (A) BMMCs transduced with mLMIR5 were stimulated with either control IgG or anti-mLMIR5 Ab for 3 or 15 minutes. Cell lysates were subjected to immunoblotting with either anti–phospho-p44/42 MAPK (pERK1/2), anti–phospho-p38 MAPK (pp38), or anti–phospho-Akt (pAkt) Ab. Equal loading was evaluated with by reprobing the immunoblots with Abs specific for ERK1/2, p38, or Akt. (B) BMMCs transduced with mLMIR5 were incubated with PBS, control IgG, or anti-mLMIR5 Ab for 12 hours. IL-6, TNF-α, and MCP-1 released into the culture supernatants were measured by ELISA. (C) BMMCs transduced with mLMIR5 in FN- or FB-coated plates were stimulated with PBS, control IgG, or anti-mLMIR5 Ab for 60 minutes. Adherent cells were measured as described in "Measurement of cytokines and histamines and adhesion assay." (D) FLMCs transduced with mLMIR5 were incubated with PBS, control IgG, or anti-mLMIR5 Ab for 50 minutes. Alternatively, anti-TNP IgE-sensitized cells were incubated with TNP-BSA for 50 minutes. Histamine released in the culture supernatants was measured. (E) FLMCs transduced with mLMIR5 were incubated with either PBS, control IgG, anti-mLMIR5 Ab, or IgE (SPE-7) in the absence of IL-3. At indicated time points, cells were stained with PE-labeled annexin V to monitor apoptosis. Cells incubated in the presence of IL-3 were also analyzed. All data points correspond to the mean and the standard deviation (SD) of 4 independent experiments. Statistically significant differences are shown. $^*P < .05$.

survival effect was significant but weak in mLMIR5-transduced BMMCs stimulated by anti-mLMIR5 Ab (data not shown). Importantly, mLMIR5-transduced FLMCs in response to anti-mLMIR5 Ab stimulation efficiently released histamine and showed an antiapoptotic effect under IL-3–depleted conditions, thus demonstrating that engagement of endogenous mLMIR5 could also activate the cellular responses (Figure 4D,E).[25,39,40] Taken together, mLMIR5 functioned as an activating receptor in mast cells.

DAP12 is required for the activation induced by mLMIR5 engagement as well as the sufficient surface expression of mLMIR5 under physiologic conditions

To determine which adaptor protein was a physiologic partner of mLMIR5, we analyzed surface expression levels of mLMIR5 in BM cells or BMMCs derived from wild-type (WT), *DAP10*$^{-/-}$, *DAP12*$^{-/-}$, or *FcRγ*$^{-/-}$ mice.[20,22,23,28,29,41] As depicted in Figure 5A, surface expression levels of mLMIR5 in BM granulocytes derived only from DAP12-deficient mice were reduced when compared with those from other mice. On the other hand, surface expression levels of mLMIR5 in BMMCs were strongly or moderately reduced by DAP12 or DAP10 deficiency, respectively (Figure 5B). To further address the dependency of activating events caused by mLMIR5 aggregation on each adaptor protein, mLMIR5 was transduced into these BMMCs. The transduced cells exhibited comparable expression levels of FcεRI and c-kit in addition to transduced mLMIR5, irrespective of the deficiency of respective adaptor molecule (Figure 5C bottom row). FcεRI expression was not detectable in FcRγ-deficient BMMCs as reported (Figure 5C top row).[29,41] Importantly, DAP12- or DAP10-deficient BMMCs in response to mLMIR5 engagement exhibited negligible or weak, respectively, activation of ERK as compared with WT BMMCs (Figure 5D), in proportion to the decreased capacities of DAP12- or DAP10-deficient BMMCs to adhere to fibronectin (Figure 5E). Concurrently, we confirmed that adhesion levels caused by PMA stimulation were comparable among these transfectants, and that FcRγ-deficient BMMCs did not adhere in response to IgE because of the lack of FcεRI on the cell surface, as expected (Figure 5E). Although the deficiency of adaptor molecules did not show any morphologic difference in mast cells (data not shown), real-time PCR analysis demonstrated significantly low expression levels

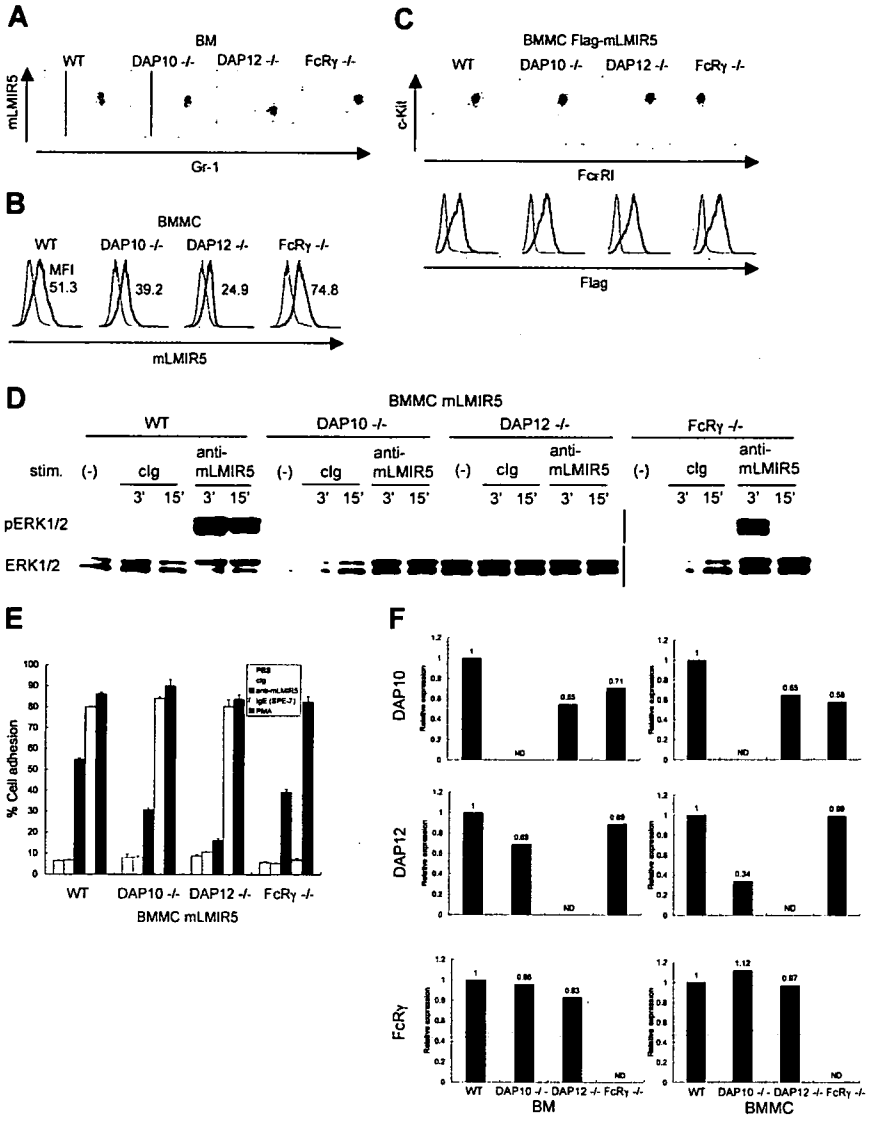

Figure 5. Analysis of BM cells and BMMCs derived from *DAP10*$^{-/-}$, *DAP12*$^{-/-}$, and *FcRγ*$^{-/-}$ mice. (A,B) Surface expression levels of endogenous mLMIR5 on BM cells and BMMCs derived from WT, *DAP10*$^{-/-}$, DAP12$^{-/-}$, or FcRγ$^{-/-}$ mice were analyzed as described in Figure 2. The mean fluorescent intensity (MFI) of mLMIR5 expression was indicated in BMMCs. (C) WT, *DAP10*$^{-/-}$, DAP12$^{-/-}$, or *FcRγ*$^{-/-}$ BMMCs transduced with Flag-tagged mLMIR5 were stained with control IgG or anti-Flag mAb followed by FITC-conjugated anti-mouse Ig Ab to confirm transduced-mLMIR5 expression levels (bottom row). Phenotypical analysis of BMMCs was performed as described in materials and methods (top row). (D) Either WT, *DAP10*$^{-/-}$, DAP12$^{-/-}$, or *FcRγ*$^{-/-}$ BMMCs transduced with mLMIR5 were stimulated with control IgG or anti-mLMIR5 Ab. The amount of phosphorylated ERK1/2 was analyzed as described in Figure 4A. Vertical lines have been inserted to indicate a repositioned gel lane. (E) Either WT, *DAP10*$^{-/-}$, DAP12$^{-/-}$, or *FcRγ*$^{-/-}$ BMMCs transduced with mLMIR5 were stimulated on FN-coated plates. Percentages of adherent cells were estimated. All data points correspond to the mean and the SD of 3 independent experiments as indicated. (F) Relative expression levels of DAP10, DAP12, and FcRγ among WT, *DAP10*$^{-/-}$, DAP12$^{-/-}$, and *FcRγ*$^{-/-}$ BM or BMMCs were estimated by using real-time PCR as described in "Gene expression analysis." The amount of expression was indicated relative to that in wild-type BM or BMMCs. Data are representative of 3 independent experiments.

(approximately 30%) of DAP12 in DAP10-deficient BMMCs and decreased expression levels of DAP10 (approximately 60%) in DAP12- or FcRγ-deficient BMMCs, when compared with those in WT BMMCs (Figure 5F right panel). On the other hand, expression levels of DAP12 in DAP10-deficient BM were approximately 70% of those in WT BM (Figure 5F left panel). Considering the recent report that DAP12 transcript levels were not altered by DAP10 deficiency,[20,22] expression levels of DAP12 might have been decreased during the course of differentiation of DAP10-deficient BMMCs in culture. Thus, attenuated activation induced by mLMIR5 cross-linking as well as reduced surface expression levels of mLMIR5 in DAP10-deficient BMMCs can be explained by the decreased expression levels of DAP12 rather than by the deficiency of DAP10. In summary, DAP12 plays a major role in maintaining surface expression levels of mLMIR5 under physiologic conditions and in transmitting activating signals induced by mLMIR5 aggregation.

Different signaling pathways between mLMIR5 and hLMIR5

To explore whether the activating functions of hLMIR5 are also regulated by DAP12, Flag-tagged hLMIR5 was transduced into WT or DAP12-deficient BMMCs. Surprisingly, DAP12 deficiency did not inhibit but rather enhanced IL-6 production caused by hLMIR5 cross-linking (Figure 6A bottom row), while it completely abrogated that by mLMIR5 cross-linking (Figure 6A top row), notwithstanding equivalent amounts of cytokine production of WT and DAP12-deficient transfectants stimulated by PMA (Figure 6A). This was consistent with the finding that LMIR5 cross-linking induced strong activation of ERK in DAP12-deficient BMMCs transduced only with hLMIR5, but not mLMIR5 (Figure 6B), and that ERK activation induced by cross-linking of transduced hLMIR5 was rather enhanced in DAP12-deficient BMMCs in comparison with that of WT BMMC (Figure 6C). Since hLMIR5, but not mLMIR5, contained the putative phosphorylation site (Y188) in the cytoplasmic tail, we asked if this is related to DAP12-independent activation of mast cells stimulated by hLMIR5 cross-linking. Intriguingly, the phosphorylation of hLMIR5 was observed only in DAP12-deficient, but not WT, mast cells in response to hLMIR5 aggregation (Figure 6C). To further confirm that Y188 of hLMIR5 was indeed phosphorylated, we transduced either mock, Flag-tagged hLMIR5, or Flag-tagged hLMIR5 (Y188F) into WT BMMCs. As demonstrated in Figure 6D, stimulation of BMMCs with pervanadate induced tyrosine phosphorylation of hLMIR5, but not hLMIR5 (Y188F), suggesting that Y188 was a

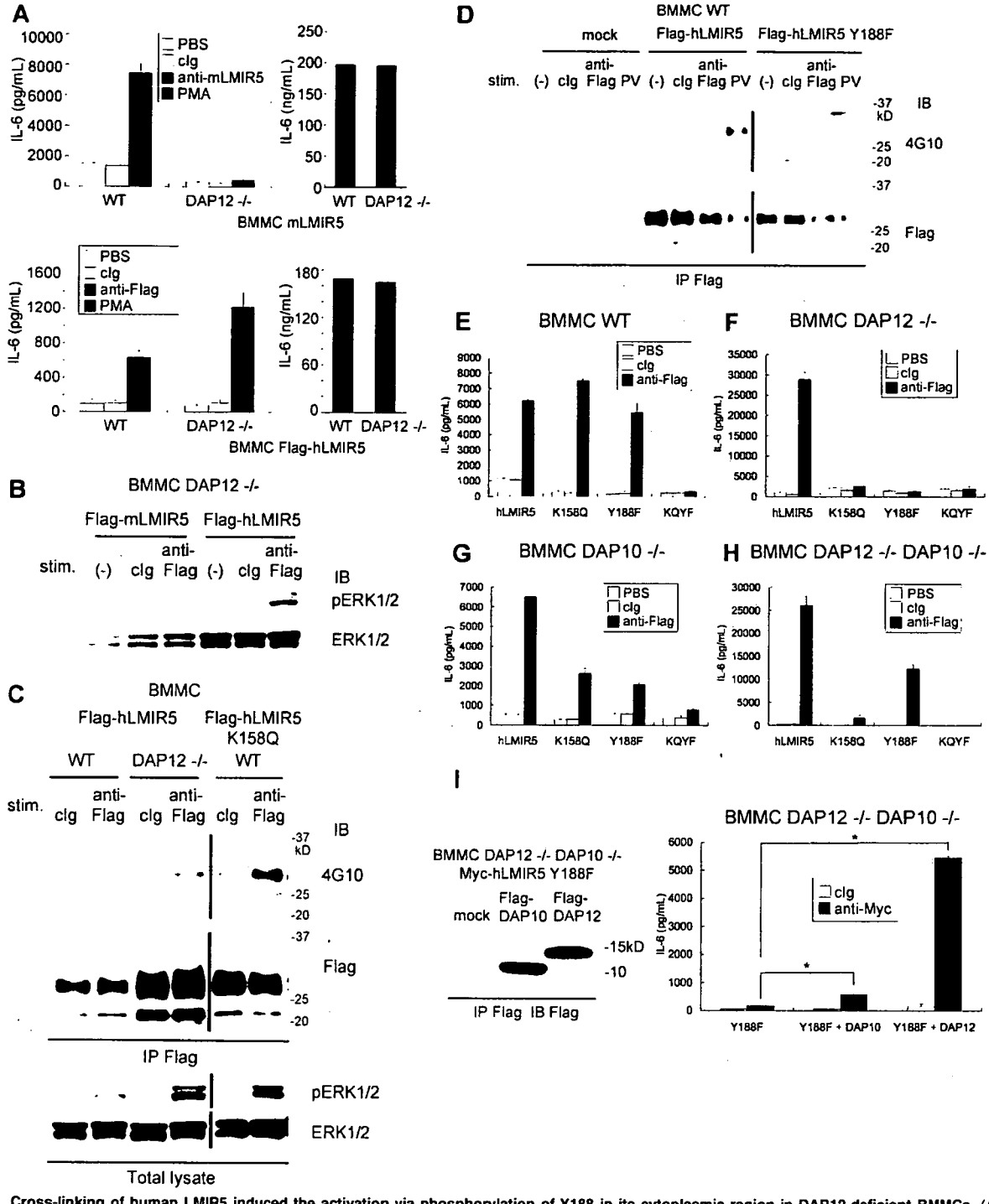

Figure 6. Cross-linking of human LMIR5 induced the activation via phosphorylation of Y188 in its cytoplasmic region in DAP12-deficient BMMCs. (A) WT or *DAP12*$^{-/-}$ BMMCs transduced with a Flag-tagged mLMIR5 were stimulated with control IgG, anti-mLMIR5 Ab, or PMA (top panels), while WT or *DAP12*$^{-/-}$ BMMCs transduced with Flag-tagged hLMIR5 were stimulated with control IgG, anti-Flag mAb, or PMA (bottom panels). IL-6 released into the culture supernatants was measured by ELISA. All data points correspond to the mean and the SD of 4 independent experiments. (B) *DAP12*$^{-/-}$ BMMCs transduced with either a Flag-tagged mLMIR5 or hLMIR5 were stimulated with the indicated Abs for 3 minutes. The amount of phosphorylated ERK1/2 was analyzed as described. (C) WT or *DAP12*$^{-/-}$ BMMCs transduced with Flag-tagged hLMIR5 or WT BMMCs transduced with Flag-tagged hLMIR5 (K158Q) were incubated with the indicated Abs. Immunoprecipitates of cell lysates with anti-Flag mAb were immunoblotted with anti-phosphotyrosine mAb (4G10) or anti-Flag mAb. Total cell lysates were also analyzed to detect the amount of phosphorylated ERK1/2. Vertical lines have been inserted to indicate a repositioned gel lane. (D) BMMCs transduced with Flag-tagged hLMIR5, hLMIR5 (Y188F), or mock were stimulated with the indicated Ab for 3 minutes or with 100 μm pervanadate (PV) for 10 minutes. Immunoprecipitates of cell lysates with anti-Flag mAb were blotted with antiphosphotyrosine mAb (4G10) or anti-Flag mAb. Vertical lines have been inserted to indicate a repositioned gel lane. (E-H) WT (E) or *DAP12*$^{-/-}$ (F) *DAP10*$^{-/-}$ (G), or *DAP12*$^{-/-}$*DAP10*$^{-/-}$ (H) BMMCs transduced with Flag-tagged hLMIR5, hLMIR5 (K158Q), hLMIR5 (Y188F), or hLMIR5 (K158Q) (Y188F) were stimulated with control IgG or anti-Flag mAb. IL-6 released into the culture supernatants was measured by ELISA. All data points correspond to the mean and the SD of 3 independent experiments. K158Q, Y188F, or KQYF indicate hLMIR5 (K158Q), hLMIR5 (Y188F), or hLMIR5 (K158Q) (Y188F), respectively. (I) *DAP12*$^{-/-}$*DAP10*$^{-/-}$ BMMCs transduced with Myc-tagged hLMIR5 (Y188F) were transfected with Flag-tagged DAP10, DAP12, or mock. Immunoprecipitates of cell lysates were immunoblotted with anti-Flag mAb (left panel). These cells were stimulated with control IgG or anti-Myc mAb. IL-6 released into the culture supernatants was measured by ELISA. All data points correspond to the mean and the SD of 3 independent experiments. Statistically significant differences are shown. *$P < .05$.

major phosphorylation site in hLMIR5 (Figure 6D). Interestingly, when hLMIR5 (K158Q)–transduced WT BMMCs were stimulated by hLMIR5 cross-linking, hLMIR5 (K158Q) was strongly phosphorylated (Figure 6C), suggesting that hLMIR5-mediated Y188 phosphorylation could be induced by adaptors that associate with hLMIR5 not through K158. To clarify whether phosphorylation of Y188 is required for cytokine production of mast cells caused by hLMIR5 engagement in the presence or absence of DAP12, we transduced hLMIR5 or hLMIR5 (Y188F) into DAP12-deficient BMMCs as well as WT BMMCs. As depicted in Figure 6E,F, the replacement of Y188 with phenylalanine (F) had no effect on cytokine production of WT BMMCs in response to anti-Flag mAb stimulation (Figure 6E), but abrogated that of DAP12-deficient BMMCs (Figure 6F). Altogether, these data strongly suggest that downstream of hLMIR5 there exists Y188 phosphorylation–independent and –dependent pathways in the presence and absence of DAP12, respectively.

Since DAP10 also associated with hLMIR5, we next examined the role of DAP10 in hLMIR5-mediated cytokine production of BMMCs. After hLMIR5 or hLMIR5 (Y188F) was transduced into either DAP10- or DAP10/DAP12 double-deficient BMMCs, similar experiments were performed. Surprisingly, cross-linking of hLMIR5 induced cytokine production even in the absence of both DAP12 and DAP10, suggesting the existence of unidentified adaptors of hLMIR5 (Figure 6H). Disruption of Y188 reduced, but did not abrogate, cytokine production of DAP10/DAP12 double-deficient BMMCs, indicating the existence of Y188 phosphorylation–independent and –dependent signaling pathways (Figure 6H). Transduction of DAP10 or DAP12 into hLMIR5 (Y188F)–expressing DAP10/DAP12-double deficient BMMCs enhanced cytokine production weakly or strongly, respectively, suggesting that DAP12 mainly contributed to Y188 phosphorylation–independent signaling (Figure 6I). To further characterize adaptors of hLMIR5, we examined if the replacement of K158 affected hLMIR5-mediated cytokine production. Intriguingly, the disruption of K158 did not affect cytokine production of WT BMMCs, but dampened that of DAP12-deficient BMMCs, while the disruption of both K158 and Y188 completely abrogated cytokine production irrespective of the absence of DAP10 or DAP12 (Figure 6E-H).

Cross-linking of endogenous mLMIR5 on FLMCs induced a Syk-dependent activation, resulting in cytokine production and adhesion

As mentioned, FLMCs were strongly activated in response to transduced mLMIR5 engagement compared with BMMCs. Next, we tested whether endogenous mLMIR5 could also activate FLMCs. As demonstrated in Figure 7A, activation of ERK was detected in WT FLMCs stimulated by anti-mLMIR5 Ab, but not by control Ab. This ERK activation was severely inhibited in Syk-deficient FLMCs.[27] In accordance with this, IL-6 production and adhesive property were observed only in WT but not Syk-deficient FLMCs stimulated by engagement of endogenous mLMIR5, although PMA stimulation induced comparable levels of cytokine production and adhesion between WT and Syk-deficient FLMCs (Figure 7B,C). Altogether, aggregation of endogenous mLMIR5 in FLMCs induced Syk-dependent activation of mast cells, resulting in cytokine production and adhesion.

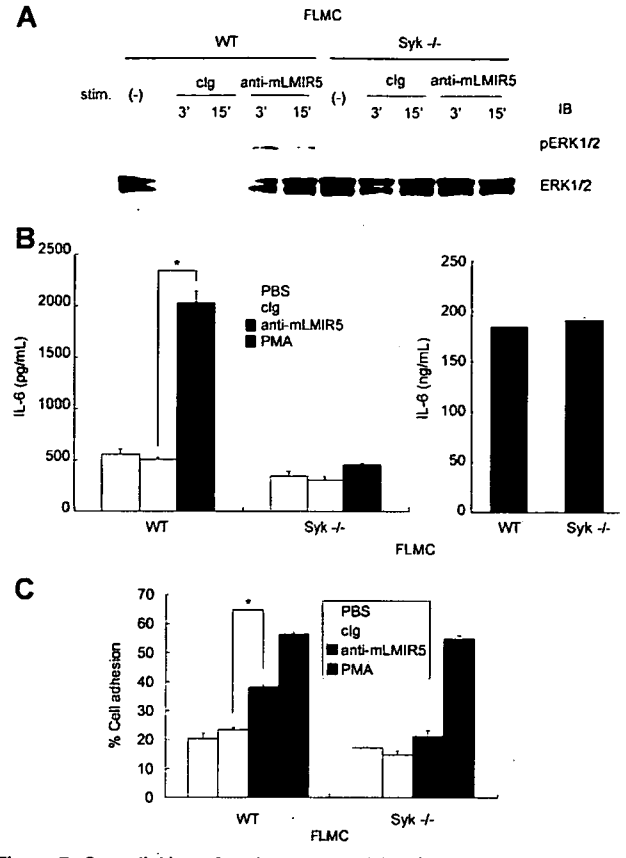

Figure 7. Cross-linking of endogenous mLMIR5 induced the activation of FLMCs. (A) WT or Syk-deficient FLMCs were stimulated with control IgG or anti-mLMIR5 Ab. The amount of phosphorylated ERK1/2 was measured as described. (B,C) IL-6 production (B) and percentage of adherent cells (C) were analyzed as described. All data points correspond to the mean and the SD of 4 independent experiments. Statistically significant differences are shown. $^*P < .05$.

Discussion

In the present study, we characterized mLMIR5/CLM-7 as a novel member of LMIRs. The structure of mLMIR5 was typical of an activating receptor. mLMIR5 showed a higher homology with the paired receptors LMIR3/CLM-1 and LMIR4/CLM-5 as compared with another pair, LMIR1/CLM-8 and LMIR2/CLM-4, in the sequence of the Ig-like domain. Accordingly, LMIR5 would function as a counterpart of LMIR3 in the absence of LMIR4. Analysis using specific Ab against mLMIR5 revealed that mLMIR5 was mainly expressed in myeloid cells like other activating LMIRs, including LMIR2 and LMIR4, although there existed several differences; for example, LMIR4 or LMIR5 was highly expressed in mature or immature granulocytes, respectively.[6,7,14] Thus, these activating receptors of the LMIR family displayed differing expression profiles among different stages of myeloid cells. In addition, high expression levels of mLMIR5 in colon and lung tissues may indicate that mLMIR5 is involved in mucosal immunity, possibly giving a clue to finding the ligands for mLMIR5.

A positively charged residue (lysine) in the transmembrane domain led us to postulate the association of mLMIR5 with ITAM- or the related activating motif–bearing adaptor proteins.[15-19,23,42] Our data indicated that mLMIR5 was mainly associated with DAP12 to maintain its surface expression levels under in vivo and in vitro physiologic conditions. However, it was noted that DAP10, when overexpressed, up-regulated mLMIR5 at surface expression